Abstract

As a consequence of the increased amount of human-generated greenhouse gas emissions, the EU has decided to reduce the CO2-emissions by 80% from 1990 levels until 2050. The European power system is believed to contribute significantly, potentially becoming completely decarbonized by 2050. Optimization modeling is used for guiding policymakers by calculating optimal pathways to how this may be achieved. These optimization models often includes uncertain parameters which can be difficult to quantify and the model results can thereafter be questioned. In the transition towards a decarbonized power sector, a methodology which yields reliable and stable results is therefore of great interest.

In this thesis, a case-study of three different scenario generation routines have been conducted. The routines proposes different approaches to represent the stochasticity of the renewable energy sources being used in the stochastic programming model, EMPIRE (European Model for Power system Investment with Renewable Energy). The routines have been tested for both bias and convergence using in-sample and out-of-sample stability, in addition to having performed a data analysis study on the renewable energy sources and the general performance on the scenario routines.

The motivation for studying scenario generation routines is generating scenarios which better approximates the true distribution and better understand the span of the potential costs of investing in the respective renewable power generators with uncertain production. Having models which output biased solutions may mislead policymakers by miscalculating the opportunity cost and lead to significant loss.

Sammendrag

Som en konsekvens av den økte mengden av menneskeskapte klimagassutslipp har EU besluttet å redusere CO2-utslippene med 80 % i forhold til nivået fra 1990 innen 2050. Det europeiske kraftsystemet antas å ha en betydelig innvirkning på dette ved å potensielt bli fullstendig dekarbonisert innen 2050. Optimeringsmodellering brukes for å veilede beslutningstakere ved å beregne optimale beslutningsstier for hvordan dette kan oppnås. Disse modellene inkluderer ofte usikre parametere som kan være vanskelige å kvantifisere, og modellresultatene kan dermed ofte stilles spørsmålstegn ved. I overgangen mot en avkarbonisert kraftsektor er derfor en metodikk som gir pålitelige løsninger som reduserer denne usikkerheten av stor interesse.

I denne oppgaven er det gjennomført et studie av tre forskjellige scenariogeneringsrutiner. Rutinene har ulike tilnærminger for å representere stokastisiteten til de fornybare energikildene som brukes i den stokastiske programmeringsmodellen, EMPIRE (European Model for Power system Investment with Renewable Energy). Rutinene er testet for både bias og konvergens ved bruk av in-sample og out-of-sample stabilitet, i tillegg til at det er utført en dataanalysestudie for de fornybare energikildene og den generelle ytelsen til scenariogenereringsrutinene.

Motivasjonen for å studere scenaregenereringsrutiner er å generere scenarier som bedre approksimerer den virkelige distribusjonen og bedre forstå de potensielle kostnadene ved å investere i de respektive fornybare kraftgeneratorene med usikker produksjon. Å ha modeller som gir løsninger med en bias kan villede politikere ved å feilberegne alternativkostnaden og føre til betydelig tap.

Preface

This master's thesis concludes my Master of Science in Industrial Economics and Technology Management at the Norwegian University of Technology.

The primary motivation for choosing this work has been my interest in combining statistical analysis to energy market modeling. This work has been an attractive opportunity for me to receive a better understanding to how energy market modeling is used to build up underneath investment decisions.

I would like to express my gratitude to the ones who have contributed to this thesis. I want to thank my supervisor, Professor Asgeir Tomasgard, for helpful advice and inspiring discussions. I would also like to thank PhD Candidate Stian Backe, providing valuable guidance throughout the project. A special thanks also goes to the Department for Industrial Economics and Technology Management for letting me use the Solstorm Cluster during my research period.

June 11, 2020.

Håkon Gjenstad Verås

Table of Contents

List of Tables

List of Figures

Chapter 1

Introduction

Modeling has ever since the development of mathematics been central for decision making and for gaining a better understanding of a problem. Approximating the costs for large investment projects can have have a significant impact on whether it is worth doing. Assumptions and restrictions have to be clarified for the model to yield realistic estimates. This task can be demanding as the model environment can be uncertain and difficult to quantify.

In 2011 the European Union (EU) published the document Energy Roadmap 2050 which outlined the EUs long-term ambition towards a 80-95 % reduction in emissions from 1990-levels, and a complete decarbonization of the power sector (Commission et al., 2011). This is in line with the Paris Agreement from 2015, in which the goal is to keep the global temperature well below 2 degrees Celsius relative to pre-industrial levels and not surpass 1.5 degrees Celsius (United Nations, 2020). As seen from Figure 1.1, this is likely to require a complete removal of the GHG emissions- and a decarbonization of the Power sector, and will require huge investments into renewable generators. Optimization models can be applied here to find the optimal investment decisions under uncertainty using stochastic programming and scenario generation. This implies finding the renewable investment opportunities with the least investment cost for each country, given the respective generator efficiency for each country. Renewable generators may vary in efficiency in seasons due to geographical position and other trends which affects countries differently.

Mathematical optimization has with the rise of distributed computer systems become more popular in the recent years. Using commercial optimization frameworks such as FICO Xpress, Cplex and Gurobi, computational intensive models has become more applicable. In addition, the data available has become increasingly more accurate, which in return makes the model output correspondingly more reliable. This makes it possible to estimate planning costs for large investment projects with significantly greater certainty than before.

Scenario generation is a methodology in mathematical optimization for generating a limited discrete distribution as input to a stochastic program. The purpose is to create a limited set of scenarios which reflects the underlying distribution of the stochastic model variables, which in return will yield correspondingly stable solutions. The aim of this thesis is to study how different scenario generation routines perform on the EMPIRE-model, which is a multi-horizon stochastic program that incorporates both short-term and long-term system dynamics and operational uncertainty (Skar et al., 2016). The model minimizes investment costs while restricting the power sector to be completely decarbonized by the end of the last investment period.

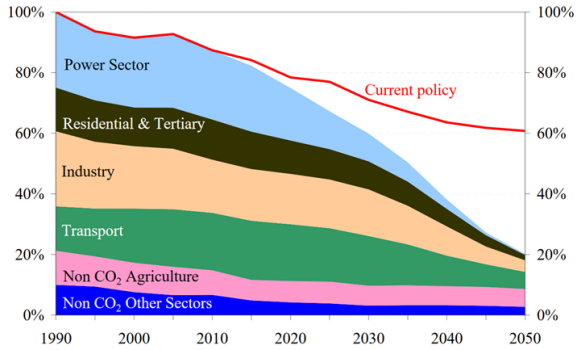

Figure 1.1: EU GHG emissions towards an 80% reduction domestic reduction relative to 1990.

The thesis is structured as follows: Chapter 2 discusses relevant topics to scenario generation and modeling the European power system. Chapter 4 reviews and summarizes previous literature. Chapter 3 discusses related theoretical concepts for optimization modeling of investment decisions under uncertainty. Chapter 5 describes the problem of analyzing scenario generation routines and why it is of interest. Three different procedures for generating scenarios for EMPIRE is outlined in Chapter 6. Data visualization and computational results from the stability analysis are outlined in Chapter 7 and Chapter 8 respectively. Chapter 9 discusses the key takeaways in the results. Lastly, Chapter 10 highlights potential extensions to this thesis.

Chapter 2

Background

This chapter introduces relevant aspects for modeling the European power system. Section 2.1 gives an introduction to the system dynamics in the European energy ecosystem. Section 2.2 gives an contextual introduction to the EMPIRE model, while Section 2.3 gives a brief introduction to what scenario generation is and different ways to construct scenarios.

2.1 Power Markets

A power system consists of fundamentally three parts, as illustrated in Figure 2.1:

- The transmission grid
- Production
- Supply and Demand

The transmission grid connects producers and consumers on a national level. The production is usually located far from the consumers, which requires the transmission grid to be able to transport the electricity throughout the given region. Variations in electricity demand and production set constraints making it necessary to have sufficient capacity in the transmission grid. Trading occurs when there is an need to account for sudden changes in supply or demand. This might also be affected by the different electricity generators as they possess different characteristics regarding the ability to respond to load variation (Energifakta Norge, 2019).

The transmission grid is usually operated by a trusted entity called an transmission system operator (TSO). Due to the relative high costs of maintaining and establishing power lines compared to the market size, the TSO is usually denoted as a

natural monopoly. In addition, the TSO is usually subjected to regulation. As an example, the TSO in Norway is Statnett.

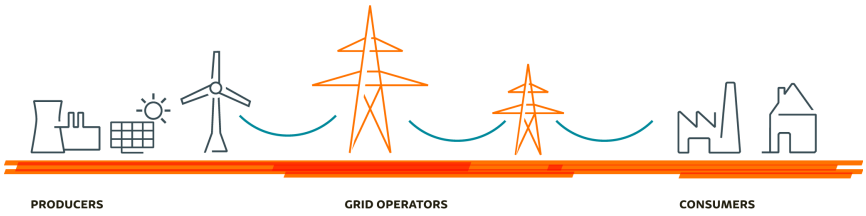

Figure 2.1: Illustration of how the electricity market is usually structured(50 Hertz, 2020).

2.1.1 The European Power System

The European power system has evolved and become more interconnected since 1951, when the Union for the Coordination of Production and Transmission of Electricity (UCPTE) started to coordinate the operational and planning recommendations for companies in Switzerland, France and Germany (ENTSO-E, 2018). The goal has originally been to ensure a reliable supply of electricity on the continental Europe, but has grown over the years to include other countries such as the United Kingdom, Iceland and Cyprus as well.

Today, the European power system consist of a synchronous grid which was previously called Union for the Coordination of Transmission of Electricity (UCTE). This became in 2008 part of the European Network of Transmission System Operators for Electricity (ENTSO-E) at the same time as the Third Energy Package was introduced (European Commission, 2019). This grid connects together a total of 42 transmission system operators (TSOs) from 35 different countries (ENTSO-E, 2019). The goal is to liberalize the gas and the electricity market in and outside of the borders of the EU, with the goal of achieving a 10% electricity interconnection between the countries (ENTSO-E, 2015). This is believed to contribute to more affordable electricity prices in Europe as a whole, as it will result in better market efficiency and higher electricity supply security (Commission, 2015).

The European power market is currently undergoing big changes with attempting to decarbonize the power sector, in line with their ambition to reduce their greenhouse gas emission with 85-90% relative to 1990-levels. Figure 2.2 shows that carbon heavy fuel such as coal, lignite, oil and natural gas represents around 43% of the current electricity production in Europe. This will require larger investments into both renewable and nuclear generators, and some studies have estimated the costs for EU to range between 139 and 633 $€_{2010}$(Jägemann et al., 2013).

The electricity grid consists of three layers: the transmission grid, the regional grid and the distributed grid. The transmission grid connects producers and consumers across different regions within the country, in addition to connect the transmission

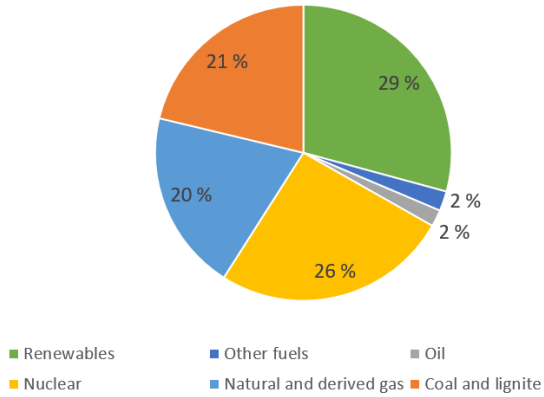

Figure 2.2: Distribution of the electricity production in Europe for 2016(European Environment Agency, 2020).

Table 2.1: Overview of the three types of layers in the Norwegian power grid(Energifakta Norge, 2019).

Grid type	Voltage (kV)	Length (km)
Distribution layer	0-22	100,000
Regional layer	33-132	19,000
Transmission layer	300-420	11,000

grid from other European countries. The regional grid and the distributional grid connects the retail consumers to the grid. The characteristics for the different layers in Norway can be seen in Table 2.1. Note that the distribution layer is significantly longer than both the regional and the transmission layer. This is because the distribution layer is less centralized and needs more branching in order to connect every households to the regional grid.

2.1.2 Balancing Supply and Demand

Today different energy sources generate various amount of electricity at different points in time. As storage capacity might not always be available, the supply can either be greater or less than the current demand. When the supply is less than the demand, it is known as load shedding. Load shedding is a controlled removal of the demand in different parts of the grid, which implies a black-out. This may impact critical parts of society such as hospitals, communication and transportation systems and is therefore highly undesirable. When some supply can not be injected into the grid it is known as curtailment. Curtailment is the effect of reducing the output of a generator and has been common since the beginning of the electric power industry. This makes seasonal production from wind and solar power potentially less efficient if there is no storage technology available.

Solar energy is commonly known for having a daily trend with more solar energy generated during the day, in addition to generating more during the summer months. Wind, on the other hand, is usually more effective during winter months. These complementary characteristics is demonstrated in Subsection 7.3 in the chapter on data analysis.

2.2 The EMPIRE Model

The EMPIRE model is a capacity expansion model which aims to find the optimal capacity investment in the European power system over medium to long-term planning horizon ranging between 20 to 50 years (Skar et al., 2016). The model consists today of 31 European countries represented by nodes which are connected by a total of 55 arcs, as seen in Figure 2.3. The list of included countries is shown in Table 2.2. The model is equivalent to maximizing the economic surplus, which is common when studying perfectly competitive markets. The model combines both short-term and long-term system dynamics with and optimizes investments under operational uncertainty(Skar et al., 2016).

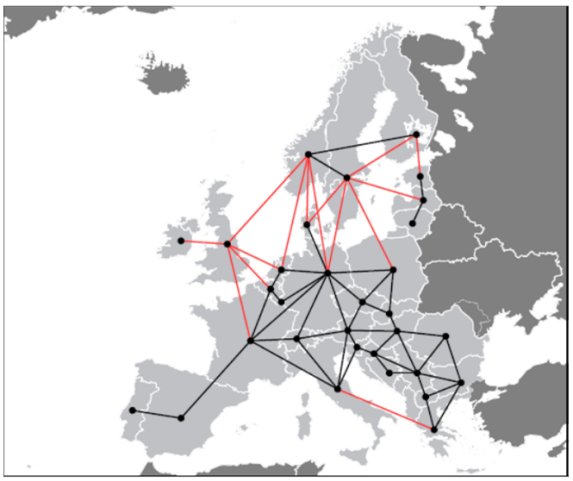

Figure 2.3: Map displaying the country nodes and the corresponding arcs for the EMPIRE-model. Red arcs represents transmission by high-voltage direct current (HVDC) and black arcs that represents transmission by high-voltage alternating current (HVAC).

There are several underlying assumptions for the EMPIRE-model(Christian Skar, Gerard Doorman and Asgeir Tomasgard, 2014):

- Perfect competition between the power producers.
- The generation capacity are aggregated for each country per technology.
- The investments are linear and continuous.
- The arcs in the transportation network are independent.

- The demand is inelastic.
- Perfect foresight about fuel prices, carbon price and load development.

The complete formulation for the EMPIRE-model can be found in Appendix A and is credited to Ph.D. Candidate Stian Backe at Department of Industrial Economy and Technology Management at NTNU.

Other approaches for modeling power markets exist as well (Ringkjøb et al., 2018). Python for Power System Analysis (PSA) is a toolbox that considers time-horizon of one year, compared to 40-50 years for EMPIRE, while the investment decisions are taken on a hourly basis. The Integrated MARKAL EFOM System (TIMES) is a general framework for modeling energy systems over long-term, multiple period time-horizons. Similar to EMPIRE, short-term decision modeling is not taking future decisions into account. Another model is the European Energy Market Model (E2M2) which implements a linear stochastic program which takes variable renewable energy sources into account (Spiecker and Weber, 2014). The investments for E2M2 are however myopic, while for EMPIRE the operational decision are made under short-term perfect foresight.

Table 2.2: Countries involved in the EMPIRE-model.

Country Code	Country
AT	Austria
BA	Bosnia H.
BE	Belgium
BG	Bulgaria
CH	Switzerland
CZ	Czech R.
DE	Germany
DK	Denmark
EE	Estonia
ES	Spain
FI	Finland
FR	France
GB	Great B.
GR	Greece
HR	Croatia
HU	Hungary
IE	Ireland
IT	Italy
LT	Lithuania
LU	Luxemb.
LV	Latvia
MK	Macedonia
NL	Netherlands
NO1	East Norway
NO2	South Norway
NO3	Mid-Norway
NO4	North Norway
NO5	West Norway
PL	Poland
PT	Portugal
RO	Romania
RS	Serbia
SE	Sweden
SI	Slovenia
SK	Slovakia

2.3 Scenario Generation

Generating scenarios means creating representations which reflects likely outcomes of random variables in the data distribution. In most cases, random variables tend to follows a continuous distribution which is difficult applying to a stochastic program. A scenario generation routine creates a discrete distribution, constisting of several scenarios, which is denoted as a *scenario tree*. This can be viewed as extracting the most core fractions of the stochastic distribution. An example of a scenario tree can be seen in Figure 2.4. A good scenario generation routine captures the most important characteristics and yields correspondingly stable results for the mathematical program. Thus, the success of a given scenario generation routine is essentially dependent on the problem modeled by the stochastic program and its representation of random variables.

Creating a good scenario generation routine might include capturing different relations between features of random variables such as correlations and anticorrelations. These relations can in some cases already be concluded from prior observations. For example in power market modeling, a seasonal anti-correlation between wind and solar is usually observed: It is more windy in the winter months compared to the summer. This anti-correlation between wind and solar have been studied in the literature for different regions, for example in (Bett and Thornton, 2016) and (Miglietta et al., 2017). Other time-dependent relations may also be accounted for, for example that the electricity consumption is higher in the evening compared to the night, and the solar irradiation is strongly periodic on a hourly scale. In addition, if a scenario is supposed to reflect a yearly distribution, prior understanding of variations within a year, such as representing each respective week, month or season could be made to make the scenario more intuitive.

2.3.1 Scenario Generation in the EMPIRE-model

The EMPIRE model have applied scenario generation for random variables such as onshore wind, offshore wind, solar, load and hydro power based on sampling historic observations of these data. Instead of using the complete historical distribution, which would have been computationally infeasible, the random variables are discretized into scenarios to be able to simulate the different outcomes due to uncertainty. The scenarios are further split up into six different seasons, aiming to capture different aspects of what is meant to portray a possible year.

The scenario generation routine for the EMPIRE-model have originally been a sampling-approach (Skar et al., 2016). Moment-matching have also been applied, which aims to make the scenarios more similar to the original distribution by finding the sample that best matches with respect to the statistical moments (Marañón-Ledesma and Tomasgard, 2019).

Other methods for generating scenarios have also been described in the literature. *Scenario reduction* attempts to minimize the scenario-tree by generating scenarios which is the closest to the initial distribution with respect to some probability

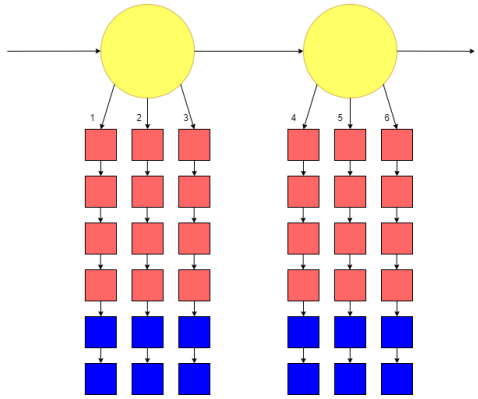

Figure 2.4: Illustration of a decision-tree in EMPIRE with a scenario-tree with three scenarios for each investment period. The yellow circles represents five-year investment periods and the red squares represents seasonal variations in the respective scenario. The blue squares represents deterministic peak seasons for the load capacity.

metric(Heitsch and Römisch, 2003). This can in some sense be viewed as a more general approach compared to Moment-Matching, as the metric for comparing the probability distributions are the statistical moments. Another possibility is to optimize the scenario tree with respect to minimizing the model, which has been called "optimal discretization" in the literature (Kaut, 2003).

Chapter 3

Theory

This chapter presents the underlying theory on the optimization modeling used in this thesis. Section 3.1 discusses stochastic programming and relevant concepts, while Section 3.2 introduces different ways to compare scenarios and stochastic distributions.

3.1 Stochastic Programming

A general two-stage stochastic linear program can be formulated as

$$\begin{array}{rlcl} z_{\text{stoch}} = \min\limits_{x} & c^T x + \sum_{i=1}^{S} p_i Q(x, \xi_j) & & \\ \text{s.t.} & Ax & = & b \\ & x & \in & \mathrm{R}^n, \end{array} \tag{3.1}$$

where

$$Q(x, \xi) = \min_{y} \{q(\xi)^T y | W(\xi) y = h(\xi) - T(\xi) x,\, y \geq 0\}$$

is the optimal solution to the second-stage problem, before the realization ξ_j has occured with corresponding probability p_j. The distribution of ξ is usually unknown which makes it often impossible to find the global optimum. This is however often solved by approximation and using discretization of possible realizations of ξ based on its assumed distribution. The stochastic solution z_{stoch} is therefore the solution to Equation 3.4. Here each scenario outcome is attached a probability $1/S$ of occurring, and the collection of all S scenarios is called a scenario tree. In this thesis it will be assumed that the probability for each scenario is equal for all scenarios. However, this may not necessarily always be the case.

3.1.1 Value of the Stochastic Solution

The value of the stochastic solution (VSS) is obtained from calculating the difference in the objective values between the stochastic and the *deterministic* solution. The deterministic solution of a stochastic program is determined by creating a deterministic program which considers only one scenario, where the stochastic variables equals their respective means. This program can be seen in

$$\begin{aligned} z_{\text{det}} = \min_{x} \quad & c^T x + Q(x, \bar{\xi}) \\ \text{s.t.} \quad & Ax = b \\ & x \in \mathrm{R}^n, \end{aligned} \tag{3.2}$$

The decision variables for the deterministic solution are then used in the stochastic program for calculating the VSS, which can be seen in

$$\text{VSS} = z_{\text{stoch}}(x_{\text{det}}) - z_{\text{stoch}}(x_{\text{stoch}}) \tag{3.3}$$

Here $z_{\text{stoch}}(x_{\text{det}})$ represents the value of the stochastic program when the decision variables is optimized for the deterministic program. For a minimization problem the VSS will always be non-negative. This reason can be intuitively understood from that the deterministic decision variables will be less optimal in the stochastic program and will therefore overestimate the objective value for a minimization problem.

3.1.2 Expected Value of Perfect Information

The expected value of perfect information (EVPI) is defined to equal the additional value of having access to perfect information in a stochastic optimization problem. The stochastic solution from Equation 3.4 is therefore compared to what is called the wait-and-see solution:

$$\begin{aligned} z_{\text{wait}} = \quad & \min_{x,y} \textstyle\sum_{i=1}^{S} p_i \left(c^T x_i + q(\xi_i^T y_i) \right) \\ \text{s.t.} \quad & Ax = b \\ & W(\xi_i) y = h(\xi_i) - T(\xi_i) x_i \qquad i = 1, \ldots, S \\ & x \in \mathrm{R}^n, \end{aligned} \tag{3.4}$$

Here x is a vector of decision variables for each respective scenario i. This can be considered as having perfect information about the outlook, where the decision variables are optimized for each respective scenario to happen. The stochastic solution will necessarily be larger for a minimization problem as the wait-and-see solution is optimized for one specific scenario at the time. The EVPI is therefore calculated to be

$$\text{EVPI} = z_{\text{stoch}}(x_{\text{stoch}}) - z_{\text{wait}}(x_{\text{wait}}) \tag{3.5}$$

Similar to the VSS, the EVPI will always be non-negative as for a given scenario, because x_{wait} consists of significantly more decision variables than x_{stoch} as the decision variables are optimized for every scenario in the wait-and-see solution. z_{wait} will therefore always be less than or equal to z_{stoch}, which on the other hand adjusts the decision variables before the stochastic variables are locked.

3.1.3 In-sample and out-of-sample stability

In-sample stability and out-of-sample stability tests are two measures for estimating the quality of the scenario generation routine, and shows how well the scenario generation routines yields stable solutions for the given stochastic program. The motivation for performing stability tests is to better understand how many scenarios is sufficient when performing the stochastic program.

In-sample stability checks if the scenario generation routine gives consistent results in the same model for different scenario trees. That is, given a set of K scenario trees $\bar{\xi}_k$, there exist a δ such that

$$|F(\mathbf{x}_i^*; k_i) - F(\mathbf{x}_j^*; k_j)| \leq \delta, \qquad \forall i, j \in K, \tag{3.6}$$

where x_i^* is a vector containing the optimal first stage decisions given scenario tree k_i.

Out-of-sample stability means locking the investment decisions for a scenario generation routine and see how well the stochastic program performs on the true underlying distribution. This means, given some fixed δ, for all realizations x_i^* of a scenario realization k_i, we have that

$$|F(x_i^*; k) - F(x_j^*; k)| < \delta, \qquad \forall i, j \in K, \tag{3.7}$$

where k represents the true underlying distribution. This is significantly more difficult than showing in-sample-stability as it is difficult knowing the true underlying distribution. Since the true stochastic distribution is usually not known, EMPIRE uses historical data as an approximation for the true distribution. However, climate may develop in a way that may deviate significantly from past observations, or the society can develop in a way that causes future load values to deviate from historical values. Given enough randomly sampled scenarios it will eventually converge to the approximated stochastic distribution.

3.2 Comparing probability distributions

A lot of different metrics with various complexity exists to measure and compare distributions (Rachev, 1991, pp. 5–7). However, many test statistics for comparing probability distributions assume that the dataset is univariate. Common tests are Shapiro-Wilk test, Anderson-Darling test and the Kolmogorov-Smirnov test, but will only be described briefly as it has not been applied and are usually already implemented in programming libraries.

The Anderson-Darling test is based on empirical distribution functions and checks whether sample data is drawn from a specific distribution. The test-statistic can be written as

$$n \int_{-\infty}^{\infty} (F_n(x) - F(x))^2 w(x)\, dF(x), \tag{3.8}$$

where $w(x)$ is a weighting function, $F(x)$ is the hypothetical distribution and $F_n(x)$ is the sample distribution.

The Kolmogorov-Smirnov test considers the sample of random variables $X_1, ..., X_n$ which are considered under the null-hypothesis to have the cumulative distribution function $F(x)$. The test statistic is then calculated as

$$D_n = \sup_x \|F_n(x) - F(x)\|, \tag{3.9}$$

where F_n is the cumulative sample distribution for $X_1, ...X_n$. It was proved in 1933(Kolmogorov-Smirnov et al., 1933) that

$$P(\sqrt(n)D_n < \lambda) \to K(\lambda), \tag{3.10}$$

where $K(\lambda)$ is known as the Kolmogorov-distribution:

$$K(\lambda) = \sum_{-\infty}^{\infty} (-1)^m e^{-2m^2\lambda^2} \tag{3.11}$$

This test has also later been extended to handle bivariate distributions (Justel et al., 1997).

A metric for comparing probabiliy distribution is the Kantorowich-Wasserstein-distance. It can be used to measure the distance between two probability distributions. It is sometimes called the earth mover's distance because it is analogous to the cost of turning one of the distributions into the other one. The metric can therefore be looked upon as a mass-transportation problem, in which the problem is to minimize the mass transported from the original distribution to the scenario S.

Matching statistical moments can be used to compare distributions with respect to the different statistical central moments. The n'th central moment is defined as

$$\mu_n = E[(X - E[X])^n] = \sum_{j=0}^{n} \binom{n}{j} (-1)^{n-j} \mu'_j \mu^{n-j}, \tag{3.12}$$

where μ equals the mean of the distribution and X is the distribution. It is important to notice that μ_n will be exponential as n grows large, so it is common to consider the *standardized* moments as well:

$$\frac{\mu_n}{\sigma^n} = \frac{E[(X - \mu)^n}{\sigma^n} \tag{3.13}$$

It can be observed that the first and the second standardized moment will equal 0 and 1 respectively. It is therefore common in moment-matching to compare the *mean*, *variance*, *skewness* and *kurtosis* which is calculated the following way:

$$\text{Mean} = \mu = E[X] \tag{3.14}$$

$$\text{Variance} = \sigma^2 = E[(X - \mu)^2] \tag{3.15}$$

$$\text{Skewness} = \frac{E[(X - \mu)^3}{\sigma^3} \tag{3.16}$$

$$\text{Kurtosis} = \frac{E[(X - \mu)^4]}{\sigma^4} \tag{3.17}$$

Dividing by an order of σ^3 and σ^4 will make both skewness and kurtosis dimensionless, compared to the mean and variance which have dimension one and two respectively. Dimensionless means ratios between quantities whose dimension cancels out in the mathematical operation. Since the dimension is one for the mean and the variance, they may differ in size compared to the skewness and the kurtosis.

These moments can be used to compare a sample distribution and the underlying distribution to generate a metric which measures how much the sample distribution differs from the whole distribution with respect to these moments. For comparing subsamples of a multivariate time-series with the whole distribution, this can be extended by calculating the moments for each single sampled time-series and compare it to the corresponding complete univariate time-series. It is however necessary to sample the same indices for each univariate time-series to preserve correlation and other dependencies for the sampled multivariate time-series.

Chapter 4

Literature Review

This chapter reviews and summarizes the related literature. Section 4.1 discusses different ways of modeling power markets. Section 4.2 goes more into detail about how stochastic distributions have been modeled using scenario generation.

4.1 Power Market Modeling

This section introduces different approaches and aspects from the literature to how power markets are modeled. This includes the mathematical structure and assumptions for the model, but also different aspects related to the problem studied. Many power market models considers endogenous investments for handling uncertainty in various degree. An exogenous investment is the initial investment into a capacity development. If the investment is not sufficient for meeting the capacity demand or a constraint, the model can determine the additional investment endogenously (Association et al., 2010). Endogenous investments is therefore usually more computational intensive as they are composed of several stages.

One of the first documented power market models created for Europe is made by Richter (2011), which proposes a linear model for optimizing future development of electricity generation capacity and their dispatch in Europe, named DIMENSION. The model represents Europe as a directed graph with vertices formulated both as a sink and a source. The model is consequently restricted by the balance equations, capacity restrictions, capacity investments and power storage, in the time horizon ranging until 2050. The model is a resulting linear energy system where the objective function is the discounted sum of the different costs. The DIMENSION-model considers the net-transfer capacity between nations endogenously, while the renewable energy sources are treated exogenously.

Capros et al. (2012) models the European power market with the ambition to

reach a low-carbon economy by 2050 with a 80% emission reduction. The model, called the Price-Induced Market Equilibrium System (PRIMES), considers different scenarios with the same amount of allowable GHG emissions from 2010 to 2050 for comparability. The PRIMES model uses data supplied by Eurostat to simulate the European power system with the use of power balance for supply and demand, CO_2-emission, energy technology penetration, prices and costs (E3M Lab, 2020). The PRIMES-model considers the value of carbon as endogenous, and is estimated through a series of iterations until the cumulative emission budget is met.

Jägemann et al. (2013) model projections for the European power sector from 2020 until 2050 with the use of a linear dynamic electricity system optimization model and a total of 36 scenarios to the model. These scenarios are made up of different instances with respect to different political decisions, for example not having nuclear energy as a possible investment, and should not be considered the same as the stochastic scenarios generated for the EMPIRE-model. The cost of the implementation was considered to vary between 139 and 633 bn $€_{2010}$ increase relative to not accounting for any CO_2 reduction target. The authors note that model variables such as investment costs for Carbon Capture and Storage (CCS) and nuclear power plants possesses large degrees of uncertainty. In particular the rather large amount for nuclear energy in the final solution may therefore be questioned. Unlike in the DIMENSION-model, the renewable energy technologies is modeled as endogenous investments.

Seljom and Tomasgard (2015) compares a deterministic and a stochastic modeling approach for a case study of wind power in Denmark using the TIMES model. The results show that the stochastic approach gives lower investments into wind power and generally lower total energy system costs compared to the deterministic model results. This highlights the significance of considering the randomness in the stochastic parameters as well. The TIMES-model considers endogenous electricity prices for Denmark because they are dual values for the electricity balance equation, while the electricity demand is exogenous.

Marañón-Ledesma and Tomasgard (2019) analyzes the aspect on how how Demand Response (DR) could be implemented in a cost-efficient way for Europe by 2050. The work was conducted integrated into the EMPIRE-model, and they found that a total DR capacity at 91 GW by 2050 reduces the storage capacity with 86% and the peak plant capacities by 11%. All of the investments into DR are considered endogenous. For the original model implementation of EMPIRE described by Skar et al. (2016), all investment periods are included in a single optimization.

4.2 Generating Scenarios

Scenario generation is a common way of representing the distribution of stochastic input variables in power models, as described in 2.3. Generating scenarios intuitively be done in many different ways, for example by giving a probability weight to an expert's opinion on future events, but more methodical approaches exist that

use sampling and statistical properties. The computational effort will naturally increase with the number of scenarios considered, but is on the other hand likely to give a more adaptable solution plan for different outcomes. This Section covers how different scenario-generation routines have been applied in the literature.

Moment-matching has been more recently used for scenario generation in the last couple of centuries. Kaut and Wallace (2007) apply moment-matching to portfolio optimization of 12 different different investment assets. The moment-matching algorithm is based on expected value, standard deviation, skewness and kurtosis, in addition to the correlation matrix between the attributes. Despite having stable results, they do not suggest that moment-matching is generally a good procedure, but given enough data it yields scenario trees which passes the stability tests.

Moment-matching is also considered by Marañón-Ledesma and Tomasgard (2019), who use it to generate scenarios for the European Model for Power Investments with high shares of Renewable Energy (EMPIRE) with Demand Response. The scenarios are sampled from a database consisting of 7 years of hourly data points. A scenario tree is then generated to match the first four moments of the historical data. The application of Moment-Matching as a procedure is however not discussed in detail.

Kaut (2020) applies the Kolmogorov-Smirnov statistic to select the most optimal sequence of datapoints which matches the historical distribution. The Wasserstein-distance has also been applied for sampling scenarios from a historical distribution, but were found to scale poorly for multivariate datasets.

Random sampling-approaches is another method which can be applied when the dataset contains several attributes and it is difficult to generate scenarios which matches all relations of significance in the dataset. Skar et al. (2016) creates a total of three scenarios for the EMPIRE-model. For each scenario, a random year is chosen and 666 hours are sampled. 48 hours are sampled from each season, in addition to six 'extreme seasons' consisting of five hours each.

Seljom and Tomasgard (2019) studies the scenario-generation methodology in greater detail for the The Integrated MARKAEL EFOM System (TIMES) model. The scenario generation is focused on hourly data of Wind power from 2000 to 2014 for the two Danish Nord Pool regions. They use Sample Average Approximations (SAA) through sampling methods to generate the scenario trees, in which the scenarios contains subsets of chronologically sampled hours from each respective season of the year that preserve the correlation between the two danish regions. The author also argues that producing scenarios based on the first four moments may yield a completely different distribution than what is expected.

Estimating the quality of a scenario generation routine can with the use of stability testing as discussed in Section 3.1.3. Kaut and Wallace (2007) measures in-sample and out-of-sample stability for a moment-matching scenario generation routine applied to portfolio optimization. For that given case they argue that a scenario-tree containing less than 1000 scenarios would be not sufficient. Seljom

and Tomasgard (2019) also calculate in-sample and out-of-sample stability for the three cases of 3, 30 and 60 different scenarios and finds that 60 scenarios is sufficient for receiving both in-sample and out-of-sample stability. A more detailed study of a moment-matching scenario routine is proposed by Kaut (2020), which instead of stability-testing studies the convergence of the matching-procedure on the first four moments mean, variance, skewness and kurtosis. The study finds that the skewness and the kurtosis is converging significantly slower compared to the mean and the variance.

Chapter 5

Problem Description

In this chapter, the problem of properly handling stochastic variables as model input for EMPIRE is described. The goal is to develop a scenario generation routine which properly captures the stochasticity of the underlying input variables. A good scenario generation routine is expected to output stable result and converge with respect to both in-sample and out-of-sample stability tests, with as little bias as possible in the scenario generation routine. This work investigates different scenario generating approaches and the stability of them. Even though scenario generation is often applied in the literature, the work on analyzing the different scenario generation routines is limited.

Power markets consists of energy sources with various complementary characteristics. Among the stochastic generators, possible investment objects are solar, wind onshore, wind offshore and hydro run-of-the-river. In addition, transmission lines and non-stochastic generation and storage capacity have to expand to compensate for the increased amount electricity power into the market. The load at a given time should also be accounted for as it is stochastic in nature as well. The EMPIRE-model described in Section 2.2 will work as a test-case for investigating how the the different scenario generation routines applies to a model of this complexity.

Chapter 6

Solution Method

This chapter presents the different scenario generation routines implemented. Section 6.1 considers random sampling, which attempts to work as a baseline scenario routine. Section 6.2 applies a moment-matching for the generators, while Section 6.3 applies the same moment-matching procedure, but only on power load for the different countries.

6.1 Random sampling of scenarios

The random sampling generation routine chooses first a random year in the range of the data. The same year is sampled for solar, wind offshore and wind onshore, while a different year is chosen for load and hydro run-of-the-river as the time series are historically disjoint.

A scenario is made by the following way: Each year is divided into four different season as shown in Table 6.1. A random sample of 168 consecutive hours days are then sampled from each of these seasons. The indices for the hours are equal for all of the generators and the load-capacity, such that the same correlation between the different generators are captured. As load and hydro run-of-the-river are from different time periods than wind onshore, wind offshore and solar, it is however not possible to gather the correlations between these two sets.

Thereafter, two peak seasons are made. The first peak season finds the country with highest average load throughout the year and the corresponding hour with the highest load to that country. 24 hours consisting of this hour and the previous 23 hours are then sampled as the first peak season throughout the whole dataset. The complete algorithm can be seen in Algorithm 1

Algorithm 1: Random Scenario Generation

Input : Generator data d.
Load data l.
Number of scenarios Ω.
Number of investment periods I.
Number of seasonal periods S.
Regular season hours h_1.
Peak season hours h_2.

Output: Scenario data $\hat{d}$.

```
1  d̂ = [];
2  for i = 1, ..., I do
3      for i = 1, ..., Ω do
4          y = sample_random_year;
5          yearly_data_generator = d[y];
6          yearly_data_load = l[y];
7          for i = 1, ..., S do
8              i_1 = Random(0, length_of_season - h_1);
9              seasonal_scenario = yearly_data_generator[i_1:i_1+h_1];
10             d̂.append(seasonal_scenario);
11             seasonal_scenario = yearly_data_generator[i_1:i_1+h_1];
12             d̂.append(seasonal_scenario);
13         c = country_with_largest_total_load_in_y;
14         i_2 = index_with_largest_load_value_for_c in y;
15         peak_country = yearly_data generator[i_2:i_2 + h_2];
16         d̂.append(peak_country);
17         i_3 = index_with_largest_aggregated_load value_for_all_countries;
18         peak_overall = yearly_data generator[i_3:i_3 + h_2];
19         d̂.append(peak_overall);
20 return d̂;
```

Table 6.1: Separation of months into respective seasons

Month	Season
December	Winter
January	Winter
February	Winter
March	Spring
April	Spring
May	Spring
June	Summer
July	Summer
August	Summer
September	Autumn
October	Autumn
November	Autumn

6.2 Moment-matching

The Moment-matching implementation is an extension of the random sampling of scenarios based on the same scenario structure. The deterministic peak seasons stays the same, while for the regular seasons the moment-matching procedure creates N different sample periods for each season. The mean, variance, skewness and the kurtosis for each sample period is calculated and aggregated for each time-series, and the sample period which best represents the total season is chosen. For computational reasons, $N = 50$ samples have been used throughout this thesis. The implementation is found in Algorithm 2.

6.3 Moment Load-matching

The third procedure is almost identical to the Moment-matching algorithm, but matches primarily on load. The procedure is motivated for two reasons. The first reason is that load is not normalized compared to the electricity generators and could bias the other procedure. The second reason is to see how Moment-matching performs when aggregated on fewer time-series.

Algorithm 2: Moment Scenario Generation

Input : Generator data d.
Load data l.
Number of test samples N.
Number of scenarios Ω.
Number of investment periods I.
Number of seasonal periods S.
Regular season hours h_1.
Peak season hours h_2.

Output: Scenario data $\hat{d}$.

```
1  d̂ = [];
2  for i = 1, ..., I do
3      for i = 1, ..., Ω do
4          y = Sample_random_year;
5          yearly_data_generator = d[y];
6          yearly_data_load = l[y];
7          B = ∞;
8          for i = 1, ..., S do
9              M = 0;
10             best_scenario = Null;
11             for i = 1, ..., N do
12                 i_1 = Random(0, length_of_season - h_1);
13                 T = yearly data generator[i_1:i_1+h_1];
14                 M = M + ‖Mean(T) − Mean(yearly_data _generator)‖;
15                 M = M + ‖Var(T) − Var(yearly_data_generator)‖;
16                 M = M + ‖Skew(T) − Skew(yearly_data_generator)‖;
17                 M = M + ‖Kurt(T) − Kurt(yearly_data_generator)‖;
18                 if M < B then
19                     B = M;
20                     best_scenario = seasonal_scenario;
21             d̂.append(best_scenario);
22         c = country_with_largest_total_load_in_y;
23         i_2 = index_with_largest_load_value_for_c_in_y;
24         peak_country = yearly_data generator[i_2:i_2 + h_2];
25         d̂.append(peak_country);
26         i_3 = index_with_largest_aggregated _load_value_for_all_countries;
27         peak_overall = yearly_data generator[i_3:i_3 + h_2];
28         d̂.append(peak_overall);
29 return d̂;
```

Chapter 7

Data Analysis

This chapter discusses first how the data is retrieved and preprocessed in Section 7.1 and Section 7.2. Lastly, Section 7.3 gives insight into how the data is structured and visualizes how a moment-matching procedure attempts to model an underlying distribution.

It should be emphasized that for the moment-matching scenarios in this chapter and the Computational Study is using the *central moments* described in Section 3.2 for comparing the scenarios. This might have impact the results in the sense that the moments are weighted differently as they are of different dimensions and is therefore not equally scaled. Due to time-constraints, the chapter on the Data Analysis and the Computational Study has not been reiterated.

7.1 Data Gathering

Load data

Five years of quarterly data of load has been gathered for the different countries in the EMPIRE-model for the five years 2015 until 2019 using Simple File Transfer Protocol from the ENTSO-E-initiative(ENTSOE, 2020). This have been reduced to hourly data by removing data points which are not integer hours as the variation in load in between hours is small and were considered easier to implement compared to taking the mean of the four datapoints in each hour. The remaining data points have thereafter been grouped by hour and landcode and then summed up. This is because some countries may be divided into different areas as well.

Missing data has been replaced with the yearly mean for each respective country's load, and the five-year mean has been used if the whole year is missing. Quarterly or monthly mean could also have been applied, but the ambition has been to only

remove the extreme outliers and not necessarily fit them into the seasonal variations of the dataset. This will replace the outliers with the yearly mean and might still deviate from the seasonal trend, but can now be considered white noise as the amount of datapoints with similar characteristics have are significantly more. Regarding replacing whole years of mising data with the five-year mean, the goal has been to make the dataset as complete as possible, not removing smaller countries despite the lack of data.

Solar, Wind offshore and Wind onshore

Hourly data of solar power, wind offshore power and wind onshore power has been gathered for the years 1985 to 2015 from the Renewables.ninja-platform (Renewables.ninja). Renewables.ninja is a webtool developed at Imperial College London and ETH Zürich which gathers data from global reanalysis models and satellite observations.

Renewable.ninja has two available datasets for solar power: MERRA2 and SARAH. MERRA2 was chosen, as SARAH was considered to have some missing values. Any replacement of missing values for MERRA2 is therefore not necessary.

Hydro data

Quarterly generation data for run-of-the-river and poundage has been gathered from ENTSO-E(ENTSO-E) for the years 2015-2019. Data access requires user registration and access rights for using Simple File Transfer Protocol, which has been provided by ENTSO-E. Similar to the load data, data points which are not integer hours have been removed, and the datapoints have been grouped by hour and countrycode, and thereafter summed up.

The data has then for each country and year been divided by the yearly maximal country value to yield a metric describing how big share of the maximal production is currently being produced in a specific hour. This is for making the dataset compatible with how EMPIRE is implemented. This can also be viewed as the amount of installed capacity being used in that given hour.

7.2 Data Preprocessing

To boost the reliability of the results it is important to know that the data put into the model is not faulty or wrong. The total sum of the load among all countries between 2015 to 2019 are shown in Figure 7.1. The plot show significant deviations, which gives a clear indication of outliers in the dataset. A simple preprocessing algorithm has therefore been implemented for each country to remove the biggest outliers from the dataset.

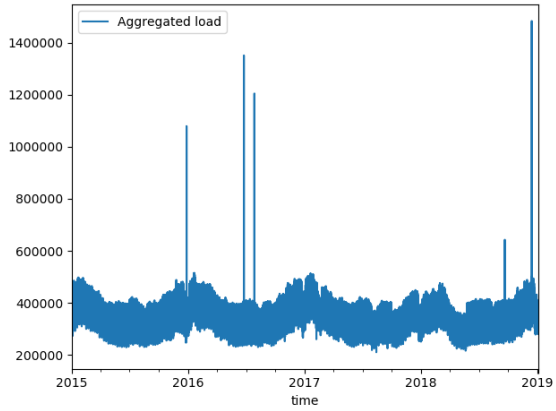

Figure 7.1: Summed up load capacity for all European countries.

The standard deviation and the median is calculated for each country, and every points deviating with more than three standard deviations from the median is considered an outlier. The use of three outliers was empirically tested as a trade-off between the number of points detected as outliers. A smaller treshold will eventually start removing seasonal datapoints as the median is calculated globally and is therefore seasonal independent. The median could have been implemented locally with a trend, but was viewed as unnecessary as the main goal has only been to remove the most significant outliers. The median is chosen instead of the mean because it is less sensitive to outliers. As some points are extreme outliers, they have a significant impact on the calculated standard deviation. The algorithm is therefore implemented as a while-loop, recalculating the standard deviation whenever an outlier is removed. An illustration for how the algorithm works is shown for both Norway and Macedonia in Figure 7.2 with corresponding pseudocode shown in Algorithm 3. For Norway the biggest outliers are removed and replaced with the median for Norway. Linear interpolation of points in the neighbourhood would also have been an possibility, but it is important to have in mind that there also exists 'less extreme' outliers in the neighbourhood, which will make the replacement-operation less predictable. In between 2015 and 2016 we see that the replacement deviates from the neighbourhood somewhat for Norway. However, reducing the treshold of three standard deviations further will eventually result in more non-outliers being replaced as well because the median is calculated globally. When the

outliers are removed for Macedonia, we see that there is still a lot of noise in the dataset. The main ambition is however to remove outliers and not filter out noise, as the outliers directly interfere with sampling out the peak-seasons discussed in Section 6.1 on generating random scenarios.

Algorithm 3: Smoothing algorithm for the load dataset

Input : Load data d.
Number of countries c.
Output: Smoothed data d.

for $i = 1, \ldots, c$ **do**
  $M_i \leftarrow \text{Median}(d_i)$;
  $\sigma_i \leftarrow \sqrt{\text{Var}(d_i)}$;
  for $j = 1, \ldots, \|d_i\|$ **do**
    if $|d[j]_i - M_i| > 3\sigma_i$ **then**
      $d[j]_i \leftarrow NaN$;
  while d_i *contains NaN-values* **do**
    for $j = 1, \ldots, \|d_i\|$ **do**
      if $|d[j]_i$ *is NaN* **then**
        $d[j]_i \leftarrow M_i$;
    $M_i \leftarrow \text{Median}(d_i)$;
    $\sigma_i \leftarrow \sqrt{\text{Var}(d_i)}$;
    for $j = 1, \ldots, \|d_i\|$ **do**
      if $|d[j]_i - M_i| > 3\sigma_i$ **then**
        $d[j]_i \leftarrow NaN$;
return d;

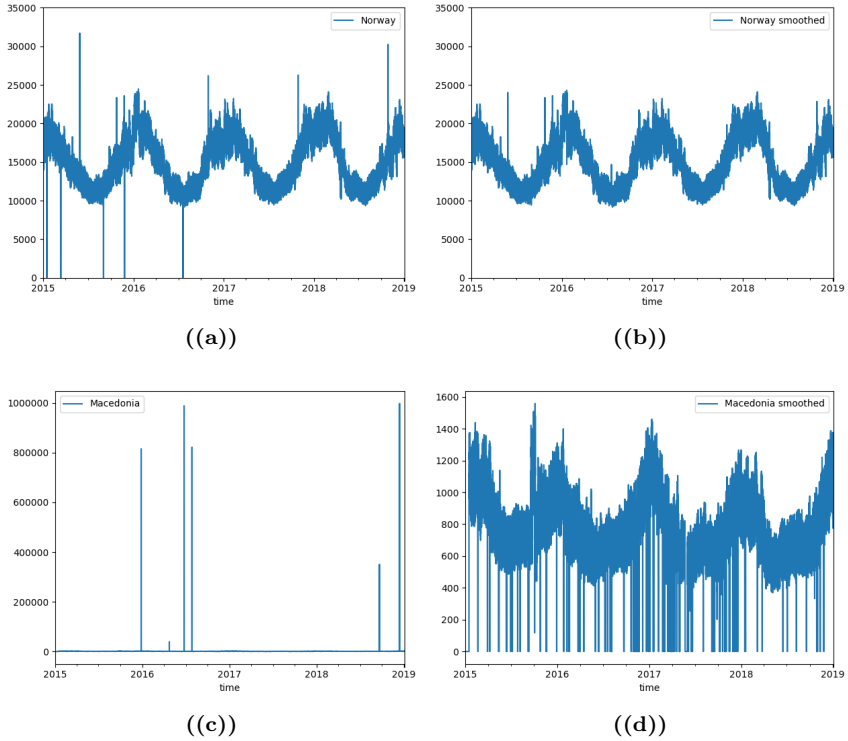

Figure 7.2: Removal of outliers for the load dataset for Norway and Macedonia.

7.3 Complementary Energy Sources

The different countries in Europe have different potential for developing solar photovoltaic, wind power and hydro run-of-the-river. The overview for the countries generator profile can be seen in Table 7.1, which shows which countries have data available for the different stochastic generators. In particular, wind offshore is naturally lacking as some countries are not located at the shore, but some countries such as Bosnia-Hercegovina and Serbia are lacking wind onshore, which may be due to either missing values or no installed capacity.

As briefly discussed in Section 2.3, there have been studies showing anti-correlation between potential wind energy and solar irradiation in different regions, see (Bett and Thornton, 2016) and (Miglietta et al., 2017). The aggregated average values for all countries for the different stochastic energy generators are shown on a monthly and hourly basis in Figure 7.3 and Figure 7.4, respectively. From the monthly aggregated data, wind onshore and wind offshore generates less power during the summer months relative to the winter months. This is in contrast to solar power that generates more power during the summer months. In addition, power from wind onshore and wind offshore are generally more volatile for each

Table 7.1: Generator profile for each of the 31 countries for the EMPIRE-model. Countries with missing data or only zero values are cross-marked.

Country Code	Country	Solar	Wind onshore	Wind offshore	Hydro run-of-the-river
AT	Austria	✓	✓	✗	✓
BA	Bosnia H.	✓	✗	✗	✗
BE	Belgium	✓	✓	✓	✓
BG	Bulgaria	✓	✓	✗	✓
CH	Switzerland	✓	✓	✗	✓
CZ	Czech R.	✓	✓	✗	✓
DE	Germany	✓	✓	✓	✓
DK	Denmark	✓	✓	✓	✓
EE	Estonia	✓	✓	✗	✓
ES	Spain	✓	✓	✗	✓
FI	Finland	✓	✓	✓	✓
FR	France	✓	✓	✓	✓
GB	Great B.	✓	✓	✓	✓
GR	Greece	✓	✓	✗	✗
HR	Croatia	✓	✓	✗	✗
HU	Hungary	✓	✓	✗	✓
IE	Ireland	✓	✓	✓	✓
IT	Italy	✓	✓	✗	✓
LT	Lithuania	✓	✓	✗	✓
LU	Luxemb.	✓	✓	✗	✗
LV	Latvia	✓	✓	✗	✓
MK	Macedonia	✓	✓	✗	✓
NL	Netherlands	✓	✓	✓	✗
NO1	Norway	✓	✓	✓	✓
NO2	Norway	✓	✓	✓	✓
NO3	Norway	✓	✓	✓	✓
NO4	Norway	✓	✓	✓	✓
NO5	Norway	✓	✓	✓	✓
PL	Poland	✓	✓	✗	✓
PT	Portugal	✓	✓	✗	✓
RO	Romania	✓	✓	✗	✓
RS	Serbia	✓	✗	✗	✓
SE	Sweden	✓	✓	✓	✗
SI	Slovenia	✓	✓	✗	✓
SK	Slovakia	✓	✓	✗	✓

month compared to solar. hydro run-of-the-river generates slightly more power in the first half year and less effective in September until November. This may be due to geographical variations or less effect from hydropower due to falling temperature. Hydro run-of-the-river is also more effective than the other generators, but also the most volatile on an annual scale.

For the hourly aggregated values shown in Figure 7.4, all generators apart from solar depends less on the hour of the day. Hydro run-of-the-river seems to have some higher output during the day, which may be due to warmer climate and ice melting. Both the output of wind onshore and wind offshore show tendencies towards being independent on the hour of the day, but it is important to highlight that this is all the countries aggregated together so the geographical nature of single countries can not be seen here.

To investigate how the hourly trend varies throughout the day for single countries, two examples in Figure 7.5 shows the aggregated average values for each hour of

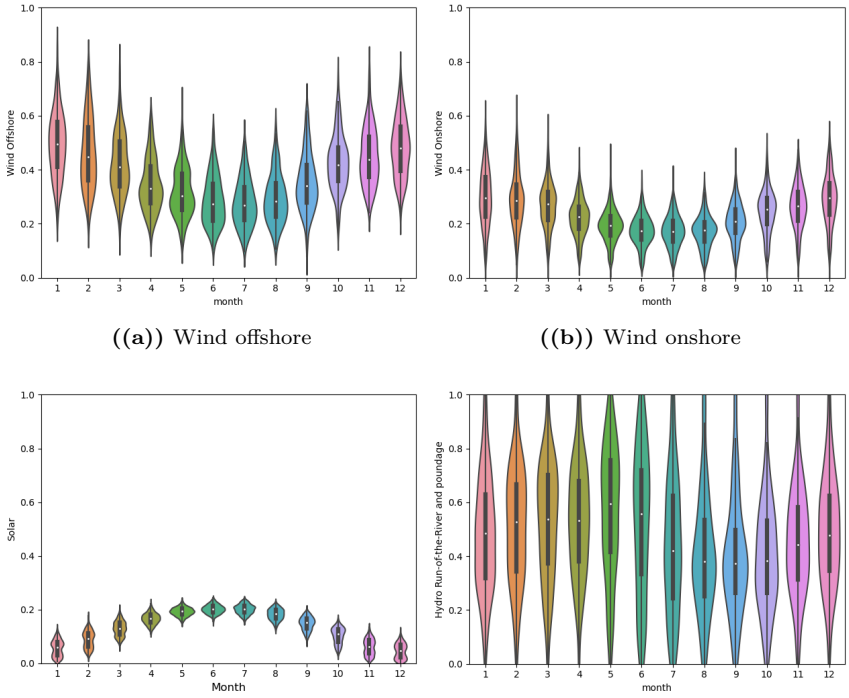

((a)) Wind offshore

((b)) Wind onshore

((c)) Solar PV

((d)) Hydro run-of-the-river

Figure 7.3: Monthly aggregated data for the different stochastic generator profiles for all European countries from their respective history of data.

the day for hydro run-of-the-river in Finland and wind offshore for France. Especially hydro run-of-the-river shows a significant increase during the day, while wind offshore has lower variance during night. This is likely due to hydro run-of-the-river includes pondage as well, and the demand for electricity is higher during the day. The corresponding aggregated average load for Finland is shown in Figure 7.6 and shows a strong relation to capacity factor for hydro run-of-the-river. These hourly seasonalities does not happen generally for all other countries, but it gives a strong indication that both wind and hydro run-of-the-river may be affected by daily seasonalities as solar. Other possible explanation can be that the daily rise and fall of temperature may affect the amount of wind and hydro available in the region.

The energy sources also have various complementary characteristics. Figure 7.7(a) and Figure 7.7(b) shows how the hourly capacity factors from solar, wind onshore and energy offshore are distributed over 30 years of data. The figures shows that the hourly capacity factors for the energy sources may differ significantly between countries. Solar seems to have generally less impact than both wind onshore and

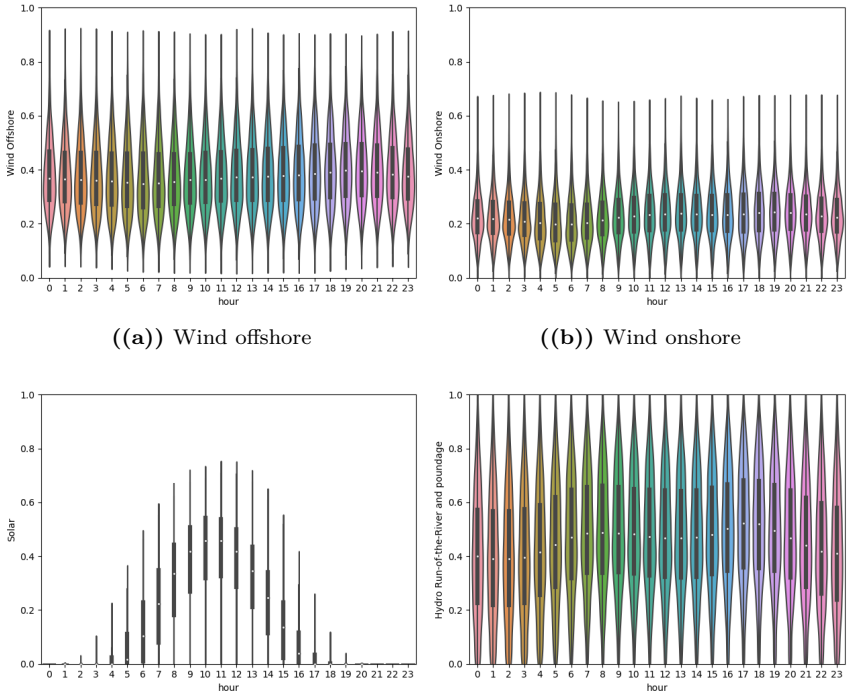

((a)) Wind offshore

((b)) Wind onshore

((c)) Solar PV

((d)) Hydro run-of-the-river

Figure 7.4: Hourly aggregated data for the different stochastic generator profiles for all European countries from their respective history of data.

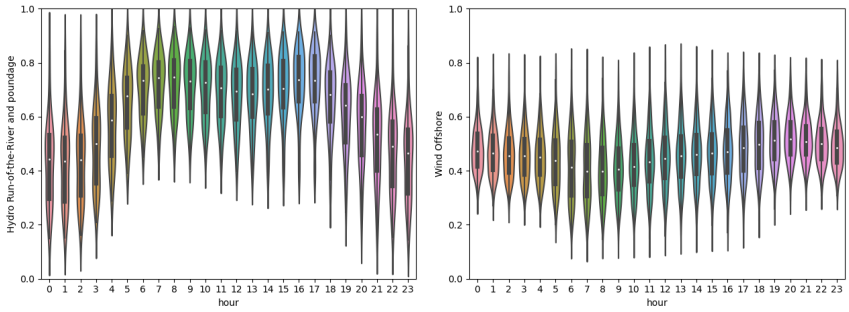

((a)) Hydro run-of-the-river

((b)) Wind offshore

Figure 7.5: Hourly aggregated data for hydro run-of-the-river for Finland and wind offshore for France.

wind offshore. On the other hand, Figure 7.8 shows that solar deviates less between

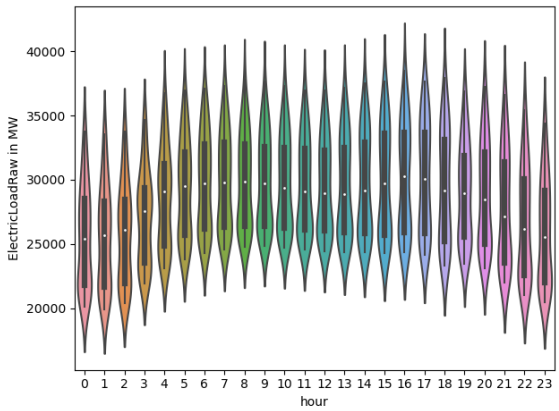

Figure 7.6: Aggregated hourly load for Finland.

years compared to wind offshore and wind onshore. This makes solar energy more predictable than the other two energy sources. In addition, none of the three energy sources show any strong tendencies towards being non-stationary between different climatic years. This makes sampling of years a suitable procedure when generating scenarios. The aggregated energy sources for weekdays can also be seen in Figure 7.9. Some but does not seem to have any impact on the renewable capacity factor.

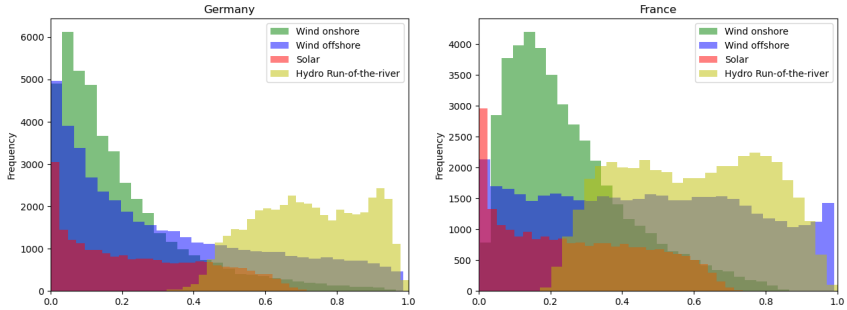

((a)) ((b))

Figure 7.7: Country generator profiles for Germany and France for the years 2001-2005, and hydro run-of-the-river for the years 2016-2020. Zero-values have been removed for visualization purposes, as it corresponds to roughly half the data points of the solar-dataset.

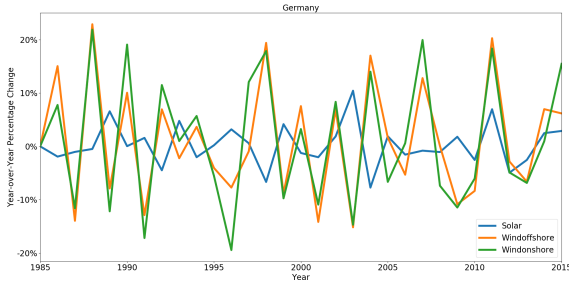

Figure 7.8: Year over year percentage change for the different energy sources for Germany.

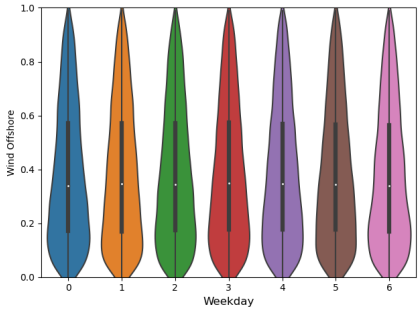

((a)) Wind offshore

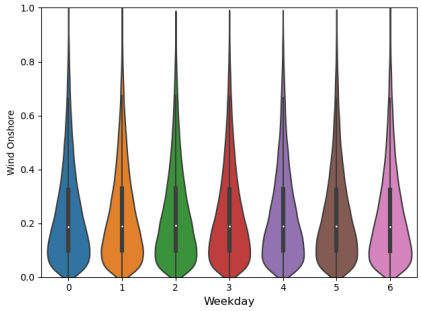

((b)) Wind onshore

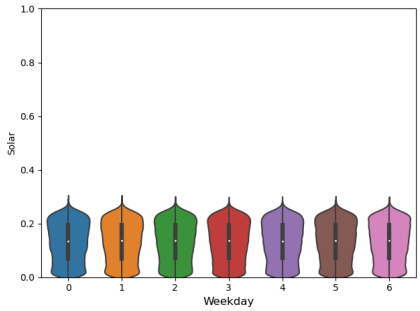

((c)) Solar PV

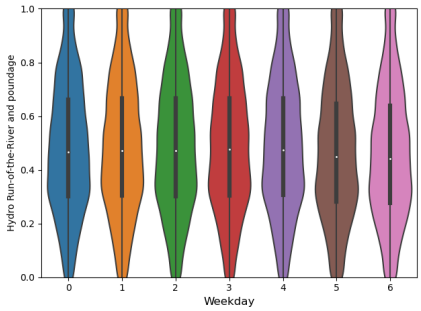

((d)) Hydro Run-of-the-River

Figure 7.9: Aggregated renewable energy sources for weekdays, where '0' is Monday, '1' is Tuesday, and so on, until '6' represents Sunday.

7.3.1 Moment-Matching Scenarios

The moment-matching procedure has been studied to see how it adapts to the underlying distribution. Figure 7.10 shows how the moment-matching scenarios with 100 samples compares to a random generated scenarios. The difference between

the approximated distribution and the seasonal distribution are shown in the for a Random routine, "Univariate" moment-matching, and a "Multivariate" moment-matching. The "Multivariate" is the combined moment-matching procedure on all of the four stochastic generators together, while the "Univariate" moment-matching only take one generator into account at a time. This is to investigate how the moment-matching procedure generalizes to several time series.

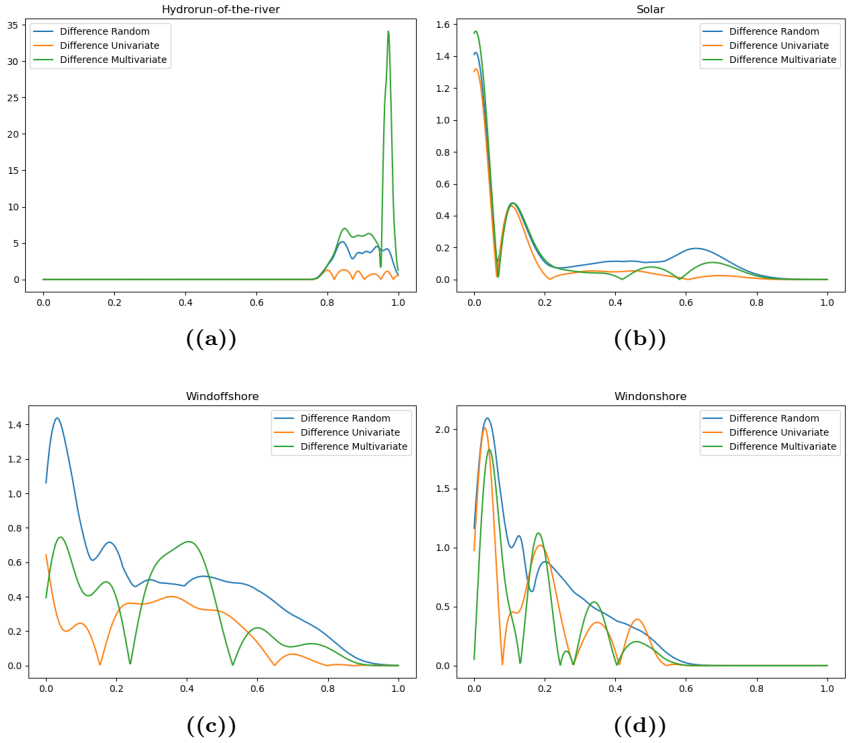

Figure 7.10: Illustration of how the different Scenario Generation Routines adapt to the Seasonal data. The data being used is Germany for the summer of 2000. For hydro run-of-the-river the year 2015 has been used instead.

For solar, the difference between the different scenario routines is almost insignificant, likely due to high seasonality in solar power on a daily basis. For wind offshore, the "Univariate" seems slightly better than both the "Multivariate" and the Random routine, while for wind onshore it is difficult to tell if a routine approximate the distribution better than the other. This is unexpected as the "Univariate" moment-matching is believed to have significant improvements over the other routines. This is however seen for hydro run-of-the-river where the "Univariate" almost fit the seasonal data perfectly, while the "Multivariate" Moment-matching procedure is clearly performing the worst, likely due to having sampled a subset which are very stable around 0.9-0.95. This shows that the Moment-matching procedure

may yield distributions which deviates somewhat from the underlying distribution. This shows that the accuracy of a moment-matching routine is likely to depend much on the data distribution as well.

The deviation from the true distribution varies between the generators as expected, as they possesses different traits with respect to seasonality which can make it difficult to obtain a good representation of the true stochastic distribution as a whole. It is however unexpected that the "Univariate" moment-matching procedure does not show any significant improvement over the Random routine. Possible explanations to this is that the moment-matching routine has been implemented that only compares the moments between the sample distribution and the true distribution as a whole. An alternative could be to compare the moments as a sum of smaller segments instead, with the aim of better match the seasonality in the distribution. As mentioned in the beginning of this chapter, the moment-matching procedure is also compared using central-moments, which is likely to give skewness and kurtosis a larger weight and override the impact from the variance and the mean. This highlights the importance of implementing the moment-matching procedure in a way that significantly converge to the true distribution.

Chapter 8

Computational Study

The computational study has been performed in Python 3.7.7. The model presented in Chapter 6 is implemented using Pyomo 5.6.8 and is solved using the Gurobi-package. All smaller computations are performed on an 2 x Intel® Xeon® Gold 5115 2.4GHz CPU with 20 cores, 40 threads and 96 GB RAM. Larger computations with more than 5 scenarios for In-Sample stability in Case 1 are performed on an 2x 3.5GHz Intel® Xeon® Gold 6144 CPU with 8 core and 384Gb RAM.

This chapter reviews different scenario generation routines with respect to In-Sample and Out-of-Sample stability testing. Section 8.1 considers a full-scale EMPIRE-model with a total of 31 different nodes, while Section 8.2 studies the best performing scenario generation routine from Section 8.1 more in detail, restricted to a subset of Europe. While the results are visualized as violin plots in this chapter, the numerical results can be found in Appendix B.

8.1 Case 1: All of Europe

The first case considers all 31 countries in Europe with 168 hours in each regular season. Due to memory problems, only a maximum of 10 scenarios for each investment period have been considered in this case. Three different scenario generation routines have been tested: Random (R), Moment (M) and Moment-Load (ML). Each routine has been tested for 3, 5, 7 and 10 different scenarios, all generating 20 different scenario trees to consider both the sample mean and the sample deviation. Out-of-Sample stability testing have been conducted on a total of 40 different scenarios, all generated with the Random routine.

The results for both the In-Sample and the Out-of-Sample stability testing can be seen in Figure 8.1. For the in-sample stability, the standard deviation is expected to decrease monotonically as the number of scenarios increases. Even the numerical

results in Appendix B can indicate to a downward trend in the relative standard deviation for all methods, it is not monotonically decreasing. For example, all routines with 5 scenarios deviates more than the routines producing 7 and 10 scenarios. This may be caused by that $N = 20$ is too few scenario trees to properly capture the downward trend, but may also be due to the difference in the number of scenarios for each routine can be too small to grasp a significant difference between them with respect to the standard deviation.

It can also be seen that for the in-sample stability that both the Moment-Matching and the Moment Load-matching routine consistently yields lower average objective values compared to the Random routine. Since both Moment-Matching and Moment-Load-Matching attempts to find the scenarios that best matches the underlying distribution, this may result in a bias in the objective value compared to the Random routine. This is also the case as the objective value in the Out-of-sample stability tests

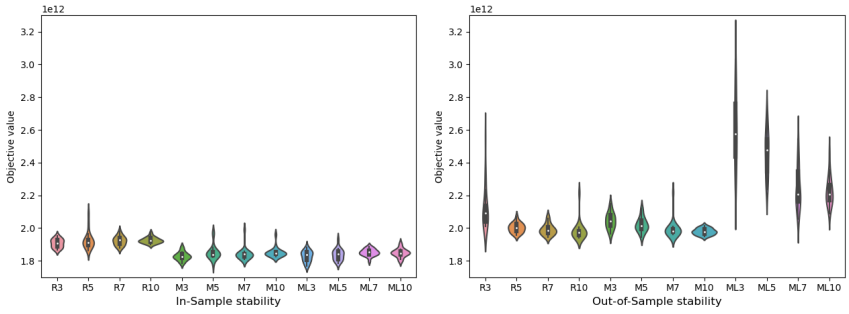

((a)) In-sample stability **((b))** Out-of-sample stability

Figure 8.1: In-sample and Out-of-sample stability for N=20 scenario trees for the different scenario generation routines.

For the Out-of-Sample stability tests, the average objective values are monotonically decreasing with increased number of scenarios for all routines, indicating that more scenarios can be used to support investment decisions that decrease the objective function further. Both Moment-Matching, and in particular the Moment-Load-Matching, show significant increase in objective value between the In-Sample and the Out-of-Sample stability tests. This indicates that both of these Scenario Generation Routines does not produce investment decisions that perform well in arbitrary scenarios.

8.2 Case 2: Subset of Europe

Case 2 explores a subset of Europe consisting of only Belgium, Germany and France, with the ambition to consider more scenarios and witness indications of convergence in the Out-of-Sample stability. Since the Moment- and the Moment Load routines

showed indications of bias in Section 8.1, only the Random routine has been considered in this case. A slight modification to the algorithm has been made so that the years sampled for solar and wind can now repeat itself in the algorithm. This makes it possible to generate more than 20 scenarios in total.

Four different variations of the Random routine have been tested. 20 scenario trees have been created four times, each containing 10 scenarios, 50 scenarios, 100 scenarios and 200 scenarios, yielding a total of 80 different scenario trees. The reduced case makes it possible to solve the model with more scenarios without running into memory problems. A total of 500 Random generated scenarios have been applied for Out-of-sample stability testing for all of the 80 different scenario trees. The results are shown in Table 8.2. The In-Sample stability testing results shows that the relative standard deviation only decrease from 0.8 % to 0.7% by using 100 instead of 50 scenarios. The average objective value is also unchanged up to three significant digits, indicating that 50 scenarios is enough for representing the stochastic variables in this case study. This can also be seen in the Out-of-Sample stability testing results. The average value is monotonically decreasing with increased number of scenarios in the trees. However, the difference between the average objective values between the In-Sample objective values and the Out-of-Sample objective values are almost identical after 50 scenarios. This is an argument for 50 scenarios being sufficient for producing investment decisions that yield stable results the reduced case.

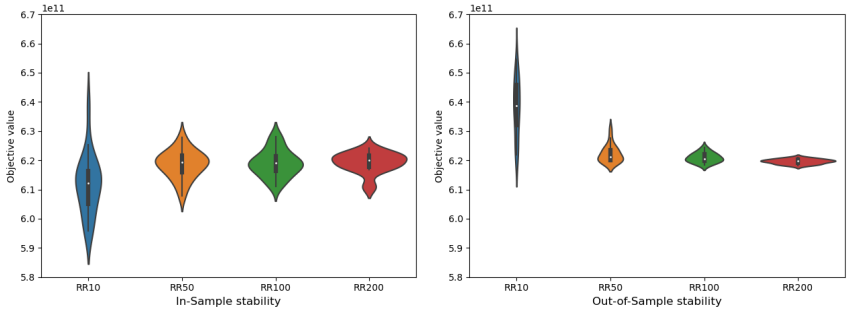

((a)) In-sample stability **((b))** Out-of-sample stability

Figure 8.2: In-sample and Out-of-sample stability tests for N=20 scenario trees for the reduced case.

Chapter 9

Concluding Remarks

In this thesis, a study on scenario generation routines have been conducted on a two-stage stochastic program supporting long-term development of power markets under short-term uncertainty. The study is motivated by the need for understanding how the scenario generation routine should be structured to better represent the stochastic parameters including electric load and the availability of renewable energy sources.. Three different variations of scenario generation routines based on sampling of historic data were proposed and compared to each other.

Before the scenario generation routines have been tested, the dataset have been preprocessed. This includes removal of outliers and replacing missing values to make the results from the scenario generation routines more stable and compatible with the dataset. In addition, the core characteristics with the stochastic parameters have been described. Solar comes off as the most volatile and the least reliable stochastic parameter on a daily basis, while hydro run-of-the-river generally has the highest average capacity factor compared to solar- and windpower. All of the renewable energy sources have some seasonality trend on a yearly basis, with hydro run-of-the-river having the least significant trend.

Two different case studies for the scenario generation routines have been considered: The full EMPIRE-model for all of Europe, and a subset considering only Germany, France and Belgium. All of the three proposed scenario generation routines have been tested for all of Europe, while for the case restricted to three countries only the Random Scenario Generation Routine have been used as the other methods were showing signs of being biased.

From the case study for all of Europe, it can be seen that the Random generation scenario shows signs of being the least biased scenario generation routine, as both Moment-Matching and Moment-Load-Matching generate objective values in which the gap between the In-Sample and Out-of-Sample stability tests deviated signifi-

cantly more compared to the Random Scenario Generation Routine. The relative standard deviation were not monotonically decreasing, which show indications that testing 20 scenario trees were not sufficient when comparing scenario generation routines with 10 scenarios or less.

For the case that only considered France, Belgium and Germany, the difference in objective value between the In-Sample and the Out-of-Sample stability tests were monotonically converging. However, the convergence is slow after 50 scenarios, reducing the gap with only $0.01 \cdot 10^{11}$ with 100 scenarios, and an additional $0.01 \cdot 10^{11}$ when considering 200 scenarios. This can be considered small when the gap-reduction from considering 10 to 50 scenarios was $0.33 \cdot 10^{11}$. The standard deviation were also shown to decrease monotonically. It is likely that this is due to stronger convergence when comparing scenario generation routines with significant difference in the number of scenarios used. This makes it reasonable to assume that 50 scenarios might be enough in the complete case as well, at least for the Random routine.

For the case that only considered France, Belgium and Germany, the difference in objective value between the In-Sample and the Out-of-Sample stability tests were monotonically converging. However, the convergence is slow after 50 scenarios, having a gap between the In-sample and the Out-of-Sample stability tests of only 0.32% relative to the average of both objective values with 100 scenarios, and an additional 0.16% when considering 200 scenarios. This can be considered small when the gap-reduction from considering 10 to 50 scenarios went from 4.2% to 0.48%. The standard deviation were also shown to decrease monotonically. It is likely that this is due to stronger convergence when comparing scenario generation routines with significant difference in the number of scenarios used. This makes it reasonable to assume that 50 scenarios might be enough in the complete case as well, at least for the Random routine.

The primary goal of this thesis has been to study the performance of different scenario generation routines applied to a two-stage stochastic program used for long-term power market modeling. It has been found that using a Random Scenario Generation Routine is less biased compared to the other Scenario Generation Routines.

Chapter 10

Future Research

This chapter discusses possible future topics which could extend this work. The aspects related to the data analysis and the theoretical foundation for the scenario generation.

With regards to future modeling, the scenario structure could be further compressed to better handle additional scenarios. A total of one week of consecutive data were used for creating the respective seasons in the scenarios. However, the strongest seasonality in the seasonal periods are between day and night, which strongly affects solar PV. It is also likely that the load differs between weekdays and regular days, even though this has not been verified in the data. A scenario generation routine which considers fractions of days instead of weeks could therefore be appropriate as long as the ratio between weekend days and regular days stays stays the same.

A challenge with generating scenarios for the EMPIRE-model is having sufficient computational memory. Hourly data could possibly be aggregated to a lower resolution, making fewer data points for representing days, weeks or months and allow for more scenarios for each investment period without increasing the computational challenge. Other ways of representing the year can be made by sampling one day for each month or week. However, such simplifications ought to be balanced with the interest in representing time series with high resolution and long duration in models like EMPIRE to represent e.g. electricity storage and ramping constraints.

It has been found that Moment-Matching can show indications of being biased. A way to possibly avoid this can be to use a hybrid approach and let a fraction of the scenarios be randomly generated, while the other fraction follows a Moment-Matching procedure. It is however important to highlight that due to the two peak seasons generated for all scenarios, the random routine can already be considered to be a hybrid approach. It is also not necessarily important to use Moment-Matching

for all generators, as generators may have a strong daily seasonality and show little to no improvement using a Moment-Matching procedure.

The Moment-Matching procedure being used calculates the different moments for the whole sample distribution at once and compares it to the underlying distribution. The matching-procedure could also be split up into several calculations and applied to smaller segments of the sample distribution with the goal of better approximating the probability distribution. The hourly or daily moments could possibly be compared to the underlying distribution to give a better approximation.

The moment-matching procedures were comparing the central moments. Another possible approach would be to transform all the statistical moments to have dimension one, as shortly described in Section 3.2. This means comparing the *mean* and *standard deviation* instead to make both metrics equal to one. Similar for skewness and kurtosis would be to let them equal their standardized moments, multiplied with the standard deviation to increase the dimension from zero to one. This is to check if comparing statistical moments with equal dimension will yield a better approximation to the distribution.

Bibliography

50 Hertz, 2020. This is 50hertz. https://www.50hertz.com/en/Company.

Association, E.W.E., et al., 2010. Powering Europe: Wind Energy and the Electrical Grid. EWEA.

Bett, P.E., Thornton, H.E., 2016. The climatological relationships between wind and solar energy supply in britain. Renewable Energy 87, 96–110.

Capros, P., Tasios, N., De Vita, A., Mantzos, L., Paroussos, L., 2012. Model-based analysis of decarbonising the eu economy in the time horizon to 2050. Energy strategy reviews 1, 76–84.

Christian Skar, Gerard Doorman and Asgeir Tomasgard, 2014. Lessons learned from building an empire. http://erpuk.org/wp-content/uploads/2015/12/7.-NUST-Skar.pdf.

Commission, E., 2015. Energy union package .

Commission, E., et al., 2011. Energy roadmap 2050. Brussels, XXX COM (2011) 885.

E3M Lab, 2020. The primes model. http://www.e3mlab.eu/e3mlab/index.php?option=com_content&view=category&id=35%3Aprimes&Itemid=80&layout=default&lang=en.

Energifakta Norge, 2019. The electricity grid. https://energifaktanorge.no/en/norsk-energiforsyning/kraftnett/.

ENTSO-E, . https://transparency.entsoe.eu/content/static_content/Static%20content/knowledge%20base/SFTP-Transparency_Docs.html.

ENTSO-E, 2015. Entso-e at a glance. https://docstore.entsoe.eu/Documents/Publications/ENTSO-E%20general%20publications/entsoe_at_a_glance_2015_web.pdf.

ENTSO-E, 2018. Union for the coordination of the transmission of electricity (ucte). https://docstore.entsoe.eu/news-events/former-associations/ucte/Pages/default.aspx.

ENTSO-E, 2019. Entso-e member companies. https://www.entsoe.eu/about/inside-entsoe/members/.

ENTSOE, 2020. Sftp guide. https://transparency.entsoe.eu/content/static_content/Static%20content/knowledge%20base/SFTP-Transparency_Docs.html.

European Commission, 2019. Third energy package. https://ec.europa.eu/energy/en/topics/markets-and-consumers/market-legislation/third-energy-package.

European Environment Agency, 2020. Overview of electricity production and use in europe. https://www.eea.europa.eu/data-and-maps/indicators/overview-of-the-electricity-production-2/assessment-4.

Heitsch, H., Römisch, W., 2003. Scenario reduction algorithms in stochastic programming. Computational optimization and applications 24, 187–206.

Jägemann, C., Fürsch, M., Hagspiel, S., Nagl, S., 2013. Decarbonizing europe's power sector by 2050—analyzing the economic implications of alternative decarbonization pathways. Energy Economics 40, 622–636.

Justel, A., Peña, D., Zamar, R., 1997. A multivariate kolmogorov-smirnov test of goodness of fit. Statistics & Probability Letters 35, 251–259.

Kaut, M., 2003. Scenario tree generation for stochastic programming: Cases from finance .

Kaut, M., 2020. Scenario generation using historical data paths .

Kaut, M., Wallace, S.W., 2007. Evaluation of scenario-generation methods for stochastic programming. Pacific Journal of Optimization 3, 257–271.

Kolmogorov-Smirnov, A., Kolmogorov, A., Kolmogorov, M., 1933. Sulla determinazione empírica di uma legge di distribuzione .

Marañón-Ledesma, H., Tomasgard, A., 2019. Analyzing demand response in a dynamic capacity expansion model for the european power market. Energies 12, 2976.

Miglietta, M.M., Huld, T., Monforti-Ferrario, F., 2017. Local complementarity of wind and solar energy resources over europe: an assessment study from a meteorological perspective. Journal of Applied Meteorology and Climatology 56, 217–234.

Rachev, S.T., 1991. Probability metrics and the stability of. Stochastic Models .

Renewables.ninja, . https://www.renewables.ninja/downloads.

Richter, J., 2011. DIMENSION-a dispatch and investment model for European electricity markets. Technical Report. EWI working paper.

Ringkjøb, H.K., Haugan, P.M., Solbrekke, I.M., 2018. A review of modelling tools for energy and electricity systems with large shares of variable renewables. Renewable and Sustainable Energy Reviews 96, 440–459.

Seljom, P., Tomasgard, A., 2015. Short-term uncertainty in long-term energy system models—a case study of wind power in denmark. Energy Economics 49, 157–167.

Seljom, P., Tomasgard, A., 2019. Sample average approximation and stability tests applied to energy system design. Energy Systems , 1–25.

Skar, C., Doorman, G., Pérez-Valdés, G.A., Tomasgard, A., 2016. A multi-horizon stochastic programming model for the european power system. Subimtted to an international peer reviewed journal, In review .

Spiecker, S., Weber, C., 2014. The future of the european electricity system and the impact of fluctuating renewable energy–a scenario analysis. Energy Policy 65, 185–197.

United Nations, 2020. The paris agreement. `https://unfccc.int/process-and-meetings/the-paris-agreement/the-paris-agreement`.

Appendix A

EMPIRE Model Formulation

This appendix shows the complete formulation of the EMPIRE-model used in this thesis. The formulation is originally contributed to Stian Backe, PhD Candidate at NTNU, Department of Industrial Economics and Technology Management.

A.1 Sets

A.1.1 Supply technology sets

$\mathcal{G}$: Set of possible generator types,
$\mathcal{T}$: Set of generator categories,
$\mathcal{B}$: Set of possible storage types.

A.1.2 Temporal sets

$\mathcal{I} = \{1, 2, ..., |\mathcal{I}|\}$: Set of investment time periods,
$\mathcal{H} = \{1, 2, ..., |\mathcal{H}|\}$: Set of operational time periods,
$\mathcal{S}$: Set of seasons.

A.1.3 Spatial sets

$\mathcal{N}$: Set of nodes,
$\mathcal{L}$: Set of bidirectional interconnectors,
$\mathcal{A}$: Set of unidirectional arcs.

A.1.4 Stochastic sets

Ω: Set of scenarios.

A.1.5 Sub-sets

$\mathcal{G}_n \subseteq \mathcal{G}$: Set of available generator types in node $n \in \mathcal{N}$,
$\mathcal{G}_t \subset \mathcal{G}$: Set of generator types in category $t \in \mathcal{T}$,
$\mathcal{G}^{\text{Ramp}} \subset \mathcal{G}$: Set of generator types limited by ramping,
$\mathcal{G}^{\text{RegHyd}} \subset \mathcal{G}$: Set of regulated hydro generator types,
$\mathcal{G}^{\text{Hyd}} \subset \mathcal{G}$: Set of all hydro generator types,
$\mathcal{B}_n \subseteq \mathcal{B}$: Set of available storage types in node $n \in \mathcal{N}$,
$\mathcal{B}^{\dagger} \subseteq \mathcal{B}$: Set of storage types with dependent ratio between energy and power,
$\mathcal{H}_s \subset \mathcal{H}$: Set of operational time periods in season $s \in \mathcal{S}$ ($\mathcal{H}_s = \{h_s^1, h_s^2, ..., |\mathcal{H}_s|\}$),
$\mathcal{H}_s^- \subset \mathcal{H}_s$: Set of operational time periods except the first in season $s \in \mathcal{S}$,
$\mathcal{A}_l \subset \mathcal{A}$: Set of unidirectional arc pair on interconnection $l \in \mathcal{L}$,
$\mathcal{A}_n^{\text{in}} \subset \mathcal{A}$: Set of arcs flowing into node $n \in \mathcal{N}$,
$\mathcal{A}_n^{\text{out}} \subset \mathcal{A}$: Set of arcs flowing out from node $n \in \mathcal{N}$.

A.2 Input data

A.2.1 Costs

$c_{g,i}^{\text{gen}}$: Cost per unit of investing in generator type $g \in \mathcal{G}$ in period $i \in \mathcal{I}$,
$c_{l,i}^{\text{tran}}$: Cost per unit of investing in interconnection $l \in \mathcal{L}$ in period $i \in \mathcal{I}$,
$c_{b,i}^{\text{storPW}}$: Cost per unit of investing in power of storage type $b \in \mathcal{B}$ in period $i \in \mathcal{I}$,
$c_{b,i}^{\text{storEN}}$: Cost per unit of investing in energy of storage type $b \in \mathcal{B}$ in period $i \in \mathcal{I}$,
$q_{g,i}^{\text{gen}}$: Cost per unit of operating generator type $g \in \mathcal{G}$ in period $i \in \mathcal{I}$,
$q_{g,i}^{\text{CO2}}$: CO2 emission factor of generator type $g \in \mathcal{G}$ in period $i \in \mathcal{I}$,
$q_{n,i}^{\text{ll}}$: Value (cost) of lost load in node $n \in \mathcal{N}$ in period $i \in \mathcal{I}$,
Q_i^{CO2}: CO2 emission ceiling for all generators in period $i \in \mathcal{I}$,

A.2.2 Technology limitations

Type dependent technology limitations

i_g^{gen}: Lifetime of investment in generator type $g \in \mathcal{G}$,
i_l^{tran}: Lifetime of investment in interconnector $l \in \mathcal{L}$,
i_b^{stor}: Lifetime of investment in storage type $b \in \mathcal{B}$,
γ_g: Ramping factor for generator type $g \in \mathcal{G}^{\text{Ramp}} \subset \mathcal{G}$,
η_a^{tran}: Efficiency factor for transmission losses along arc $a \in \mathcal{A}$, $\eta_a^{\text{tran}} \in (0,1)$,
η_b^{chrg}: Efficiency factor for charge losses with storage type $b \in \mathcal{B}$, $\eta_b^{\text{chrg}} \in (0,1)$,
η_b^{dischrg}: Efficiency factor for discharge losses with storage type $b \in \mathcal{B}$, $\eta_b^{\text{dischrg}} \in (0,1)$,
η_b^{bleed}: Efficiency factor for bleed losses with storage $b \in \mathcal{B}$, $\eta_b^{\text{bleed}} \in (0,1)$,
ρ_b: Capacity ratio between charge/discharge speed for storage type $b \in \mathcal{B}$,
β_b: Ratio between power and energy capacity for storage type $b \in \mathcal{B}^{\dagger} \subseteq \mathcal{B}$,
κ_b: Share of installed energy capacity initially available in storage type $b \in \mathcal{B}$ in each representative time period.

Node dependent technology limitations

$\bar{x}_{n,g,i}^{\text{gen}}$: Initial capacity of generator type $g \in \mathcal{G}_n$ in node $n \in \mathcal{N}$ in period $i \in \mathcal{I}$,
$\bar{x}_{l,i}^{\text{tran}}$: Initial capacity of interconnector $l \in \mathcal{L}$ in period $i \in \mathcal{I}$,
$\bar{x}_{n,b,i}^{\text{storPW}}$: Initial capacity of power of storage $b \in \mathcal{B}_n$ in node $n \in \mathcal{N}$ in period $i \in \mathcal{I}$,
$\bar{x}_{n,b,i}^{\text{storEN}}$: Initial capacity of energy of storage type $b \in \mathcal{B}_n$ in node $n \in \mathcal{N}$ in period $i \in \mathcal{I}$,
$\bar{X}_{t,n,i}^{\text{gen}}$: Max investments in generator category $t \in \mathcal{T}$ in node $n \in \mathcal{N}$ and period $i \in \mathcal{I}$,
$\bar{X}_{l,i}^{\text{tran}}$: Max investments in interconnector $l \in \mathcal{L}$ in period $i \in \mathcal{I}$,
$\bar{X}_{n,b,i}^{\text{storPW}}$: Max investments in power of storage type $b \in \mathcal{B}_n$ in node $n \in \mathcal{N}$ and period $i \in \mathcal{I}$,
$\bar{X}_{n,b,i}^{\text{storEN}}$: Max investments in energy of storage type $b \in \mathcal{B}_n$ in node $n \in \mathcal{N}$ and period $i \in \mathcal{I}$,
$\bar{V}_{t,n,i}^{\text{gen}}$: Max installed capacity of category $t \in \mathcal{T}$ in node $n \in \mathcal{N}$ and period $i \in \mathcal{I}$,
$\bar{V}_{l,i}^{\text{tran}}$: Max installed capacity of interconnector $l \in \mathcal{L}$ in period $i \in \mathcal{I}$,
$\bar{V}_{n,b,i}^{\text{storPW}}$: Max installed capacity of power of storage type $b \in \mathcal{B}_n$ in node $n \in \mathcal{N}$ and period $i \in \mathcal{I}$,
$\bar{V}_{n,b,i}^{\text{storEN}}$: Max installed capacity of energy of storage type $b \in \mathcal{B}_n$ in node $n \in \mathcal{N}$ and period $i \in \mathcal{I}$

A.2.3 Scenario input

π_ω: Probability of scenario $\omega \in \Omega$,

$\xi^{\text{gen}}_{n,g,h,i,\omega}$: Availability of generator type $g \in \mathcal{G}_n$ in node $n \in \mathcal{N}$ in period $h \in \mathcal{H}$, $i \in \mathcal{I}$ and scenario $\omega \in \Omega$,

$\xi^{\text{load}}_{n,h,i,\omega}$: Demand in node $n \in \mathcal{N}$ in period $h \in \mathcal{H}$, $i \in \mathcal{I}$ and scenario $\omega \in \Omega$,

$\xi^{\text{RegHydLim}}_{n,s,i,\omega}$: Max output from regulated hydro in node $n \in \mathcal{N}$ in $s \in \mathcal{S}$, $i \in \mathcal{I}$ and $\omega \in \Omega$,

ξ^{HydLim}_{n}: Max expected annual output from total hydro in node $n \in \mathcal{N}$.

A.3 Variables

A.3.1 Investment decision variables

$x^{\text{gen}}_{n,g,i}$: Capacity investments in generator type $g \in \mathcal{G}_n$ in node $n \in \mathcal{N}$ in period $i \in \mathcal{I}$,

$x^{\text{tran}}_{l,i}$: Capacity investments in interconnector $l \in \mathcal{L}$ in period $i \in \mathcal{I}$,

$x^{\text{storPW}}_{n,b,i}$: Capacity investments in power of storage type $b \in \mathcal{B}_n$ in node $n \in \mathcal{N}$ in period $i \in \mathcal{I}$,

$x^{\text{storEN}}_{n,b,i}$: Capacity investments in energy of storage type $b \in \mathcal{B}_n$ in node $n \in \mathcal{N}$ in period $i \in \mathcal{I}$,

$v^{\text{gen}}_{n,g,i}$: Existing capacity of generator type $g \in \mathcal{G}_n$ in node $n \in \mathcal{N}$ in period $i \in \mathcal{I}$,

$v^{\text{tran}}_{l,i}$: Existing capacity of interconnector $l \in \mathcal{L}$ in period $i \in \mathcal{I}$,

$v^{\text{storPW}}_{n,b,i}$: Existing capacity of power of storage type $b \in \mathcal{B}_n$ in node $n \in \mathcal{N}$ in period $i \in \mathcal{I}$,

$v^{\text{storEN}}_{n,b,i}$: Existing capacity of energy of storage type $b \in \mathcal{B}_n$ in node $n \in \mathcal{N}$ in period $i \in \mathcal{I}$.

A.3.2 Operational decision variables

$y^{\text{gen}}_{n,g,h,i,\omega}$: Output from generator type $g \in \mathcal{G}_n$ in node $n \in \mathcal{N}$ in period $h \in \mathcal{H}$, $i \in \mathcal{I}$ and scenario $\omega \in \Omega$,

$y^{\text{tran}}_{a,h,i,\omega}$: Power flow over unidirectional arc $a \in \mathcal{A}$ in period $h \in \mathcal{H}$, $i \in \mathcal{I}$ and scenario $\omega \in \Omega$,

$y^{\text{chrg}}_{n,b,h,i,\omega}$: Charging of storage type $b \in \mathcal{B}_n$ in node $n \in \mathcal{N}$ in period $h \in \mathcal{H}$, $i \in \mathcal{I}$ and scenario $\omega \in \Omega$,

$y^{\text{dischrg}}_{n,b,h,i,\omega}$: Discharging of storage type $b \in \mathcal{B}_n$ in node $n \in \mathcal{N}$ in period $h \in \mathcal{H}$, $i \in \mathcal{I}$ and scenario $\omega \in \Omega$,

$w^{\text{stor}}_{n,b,h,i,\omega}$: Energy content of storage type $b \in \mathcal{B}_n$ in node $n \in \mathcal{N}$ in period $h \in \mathcal{H}$, $i \in \mathcal{I}$ and scenario $\omega \in \Omega$ for demand class $d \in \mathcal{D}$,

$y^{\text{ll}}_{n,h,i,\omega}$: Amoumt of load shed in node $n \in \mathcal{N}$ in period $h \in \mathcal{H}$, $i \in \mathcal{I}$ and scenario $\omega \in \Omega$.

A.4 Objective function

$$\begin{aligned}\min z = &\sum_{i\in\mathcal{I}}(1+r)^{-5(i-1)}\times \\ &\Big[\sum_{n\in\mathcal{N}}\sum_{g\in\mathcal{G}_n} c^{\text{gen}}_{g,i}x^{\text{gen}}_{n,g,i} + \sum_{l\in\mathcal{L}} c^{\text{tran}}_{l,i}x^{\text{tran}}_{l,i} + \sum_{n\in\mathcal{N}}\sum_{b\in\mathcal{B}_n}\big(c^{\text{storPW}}_{b,i}x^{\text{storPW}}_{n,b,i} + c^{\text{storEN}}_{b,i}x^{\text{storEN}}_{n,b,i}\big) + \\ &\vartheta\sum_{\omega\in\Omega}\pi_\omega\sum_{s\in\mathcal{S}}\alpha_s\sum_{h\in\mathcal{H}_s}\sum_{n\in\mathcal{N}}\Big(\sum_{g\in\mathcal{G}_n} q^{\text{gen}}_{g,i}y^{\text{gen}}_{n,g,h,i,\omega} + q^{\text{ll}}_{n,i}y^{\text{ll}}_{n,h,i,\omega}\Big)\Big]* \qquad \text{(A.1)}\end{aligned}$$

The objective function (A.1) discounts all costs at an annual rate of r, and the investment periods are given as five year blocks. The factor $\vartheta = \sum_{j=0}^{4}(1+r)^{-j}$ scales annual operational costs to the five year investment periods.

The first four terms of (A.1) relates to investment costs in additional capacity of generation, transmission and storage. The last two terms relate to operational costs of generation and costs of load shedding. The terms for operational costs are scaled with the scenario probability π_ω and the seasonal scaling factor α_s, where α_s make sure the seasonal costs are scaled up to the length of each season.

A.5 Constraints

A.5.1 Operational constraints

Total supply from generators and storage units, as well as imports and load shedding, must be balanced with load served, exported and charged:

$$\sum_{g\in\mathcal{G}_n} y^{\text{gen}}_{n,g,h,i,\omega} + \sum_{b\in\mathcal{B}_n} \eta^{\text{dischrg}}_b y^{\text{dischrg}}_{n,b,h,i,\omega} + \sum_{a\in\mathcal{A}^{in}_n} \eta^{\text{tran}}_a y^{\text{tran}}_{a,h,i,\omega} + y^{\text{ll}}_{n,h,i,\omega} =$$
$$\xi^{\text{load}}_{n,h,i,\omega} + \sum_{b\in\mathcal{B}_n} y^{\text{chrg}}_{n,b,h,i,\omega} + \sum_{a\in\mathcal{A}^{out}_n} y^{\text{tran}}_{a,h,i,\omega}, \quad n\in\mathcal{N},\ h\in\mathcal{H},\ i\in\mathcal{I},\ \omega\in\Omega. \tag{A.2}$$

Production from generators are limited by the available installed capacity:

$$y^{\text{gen}}_{n,g,h,i,\omega} \le \xi^{\text{gen}}_{n,g,h,i,\omega} v^{\text{gen}}_{n,g,i}, \qquad g\in\mathcal{G}_n,\ n\in\mathcal{N}$$
$$h\in\mathcal{H},\ i\in\mathcal{I},\ \omega\in\Omega. \tag{A.3}$$

For thermal generators, ramping up load in between hours is limited:

$$y^{\text{gen}}_{n,g,h,i,\omega} - y^{\text{gen}}_{n,g,h-1,i,\omega} \le \gamma^{\text{gen}}_g v^{\text{gen}}_{n,g,i}, \quad g\in\mathcal{G}^{\text{Ramp}}\cap\mathcal{G}_n,\ n\in\mathcal{N},\ s\in\mathcal{S},$$
$$h\in\mathcal{H}^-_s,\ i\in\mathcal{I},\ \omega\in\Omega. \tag{A.4}$$

All storages start with an initial energy level available as a percentage of installed capacity and runs a full cycle over each representative time period in each season:

$$\kappa_b v^{\text{storEN}}_{n,b,i} + \eta^{\text{chrg}}_b y^{\text{chrg}}_{n,b,h^1_s,i,\omega} - y^{\text{discrg}}_{n,b,h^1_s,i,\omega} = w^{\text{stor}}_{n,b,h^1_s,i,\omega},\ b\in\mathcal{B}_n,\ n\in\mathcal{N},\ s\in\mathcal{S},$$
$$i\in\mathcal{I},\ \omega\in\Omega. \tag{A.5}$$
$$w^{\text{stor}}_{n,b,h^1_s,i,\omega} = w^{\text{stor}}_{n,b,|\mathcal{H}_s|,i,\omega}, \qquad b\in\mathcal{B}_n,\ n\in\mathcal{N}, s\in\mathcal{S}$$
$$i\in\mathcal{I},\ \omega\in\Omega. \tag{A.6}$$

The balance of storage is ensured between operational time steps:

$$w^{\text{stor}}_{b,n,h-1,i,\omega} + \eta^{\text{chrg}}_b y^{\text{chrg}}_{b,n,h,i,\omega} - y^{\text{discrg}}_{b,n,h,i,\omega} = \eta^{\text{bleed}}_b w^{\text{stor}}_{b,n,h,i,\omega}, \quad b\in\mathcal{B}_n,\ n\in\mathcal{N},$$
$$s\in\mathcal{S},\ h\in\mathcal{H}^-_s,$$
$$i\in\mathcal{I},\ \omega\in\Omega. \tag{A.7}$$

The energy content of storage is limited by capacity:

$$w^{\text{stor}}_{n,b,h,i,\omega} \le v^{\text{storEN}}_{n,b,i}, \qquad b\in\mathcal{B}_n,\ n\in\mathcal{N},\ h\in\mathcal{H},\ i\in\mathcal{I},\ \omega\in\Omega. \tag{A.8}$$

The amount of charging and discharging per hour is also limited by capacity:

$$y^{\text{chrg}}_{n,b,h,i,\omega} \le v^{\text{storPW}}_{n,b,i}, \qquad b\in\mathcal{B}_n,\ n\in\mathcal{N},\ h\in\mathcal{H},\ i\in\mathcal{I},\ \omega\in\Omega, \tag{A.9}$$
$$y^{\text{dischrg}}_{n,b,h,i,\omega} \le \rho_b v^{\text{storPW}}_{n,b,i}, \qquad b\in\mathcal{B}_n,\ n\in\mathcal{N},\ h\in\mathcal{H},\ i\in\mathcal{I},\ \omega\in\Omega. \tag{A.10}$$

For hydroelectric generators, energy available is restricted by season and node:

$$\sum_{h\in\mathcal{H}_s} y^{\text{gen}}_{g,n,h,i,\omega} \le \xi^{\text{RegHydLim}}_{n,i,s,\omega}, \quad n\in\mathcal{N},\ g\in\mathcal{G}^{\text{RegHyd}}\cap\mathcal{G}_n,$$
$$s\in\mathcal{S},\ i\in\mathcal{I},\ \omega\in\Omega, \tag{A.11}$$

$$\sum_{\omega\in\Omega}\pi_\omega\sum_{s\in\mathcal{S}}\alpha_s\sum_{h\in\mathcal{H}_s}\sum_{g\in\mathcal{G}^{\text{Hyd}}\cap\mathcal{G}_n} y^{\text{gen}}_{n,g,h,i,\omega} \le \xi^{\text{HydLim}}_{n}, \quad n\in\mathcal{N},\ i\in\mathcal{I}. \tag{A.12}$$

Transmission operation is in a net transfer capacity (NTC) representation:

$$y^{\text{tran}}_{a,h,i,\omega} \le v^{\text{tran}}_{l,i}, \quad l\in\mathcal{L},\ a\in\mathcal{A}_l,\ h\in\mathcal{H},\ i\in\mathcal{I},\ \omega\in\Omega. \tag{A.13}$$

Total annual emissions are limited by an emission cap:

$$\sum_{s\in\mathcal{S}}\alpha_s\sum_{h\in\mathcal{H}_s}\sum_{n\in\mathcal{N}}\sum_{g\in\mathcal{G}_n} q^{\text{CO2}}_{g,i} y^{\text{gen}}_{n,g,h,i,\omega} \le Q^{\text{CO2}}_i, \quad i\in\mathcal{I},\ \omega\in\Omega. \tag{A.14}$$

A.5.2 Investment constraints

Every generator, transmission line and storage unit have existing capacity available in each period:

$$v^{\text{gen}}_{n,g,i} = \bar{x}^{\text{gen}}_{n,g,i} + \sum_{j=i'}^{i} x^{\text{gen}}_{n,g,j}, \quad g\in\mathcal{G}_n,\ n\in\mathcal{N},\ i\in\mathcal{I},$$
$$i' = \max\{1, i - i^{\text{gen}}_g\}, \tag{A.15}$$

$$v^{\text{tran}}_{l,i} = \bar{x}^{\text{tran}}_{l,i} + \sum_{j=i'}^{i} x^{\text{tran}}_{l,j}, \quad l\in\mathcal{L},\ i\in\mathcal{I},$$
$$i' = \max\{1, i - i^{\text{tran}}_l\}, \tag{A.16}$$

$$v^{\text{storPW}}_{n,b,i} = \bar{x}^{\text{storPW}}_{n,b,i} + \sum_{j=i'}^{i} x^{\text{storPW}}_{n,b,j}, \quad b\in\mathcal{B}_n,\ n\in\mathcal{N},\ i\in\mathcal{I},$$
$$i' = \max\{1, i - i^{\text{stor}}_b\}, \tag{A.17}$$

$$v^{\text{storEN}}_{n,b,i} = \bar{x}^{\text{storEN}}_{n,b,i} + \sum_{j=i'}^{i} x^{\text{storEN}}_{n,b,j}, \quad b\in\mathcal{B}_n,\ n\in\mathcal{N},\ i\in\mathcal{I},$$
$$i' = \max\{1, i - i^{\text{stor}}_b\}. \tag{A.18}$$

There are restrictions on investments and available capacity the technologies in each node:

$$\sum_{g\in\mathcal{G}_t} x^{\text{gen}}_{n,g,i} \leq \bar{X}^{\text{gen}}_{t,n,i}, \quad t\in\mathcal{T},\ n\in\mathcal{N},\ i\in\mathcal{I}, \tag{A.19}$$

$$x^{\text{tran}}_{l,i} \leq \bar{X}^{\text{tran}}_{l,i}, \quad l\in\mathcal{L},\ i\in\mathcal{I}, \tag{A.20}$$

$$x^{\text{storPW}}_{n,b,i} \leq \bar{X}^{\text{storPW}}_{n,b,i}, \quad b\in\mathcal{B}_n,\ n\in\mathcal{N},\ i\in\mathcal{I}, \tag{A.21}$$

$$x^{\text{storEN}}_{n,b,i} \leq \bar{X}^{\text{storEN}}_{n,b,i}, \quad b\in\mathcal{B}_n,\ n\in\mathcal{N},\ i\in\mathcal{I}, \tag{A.22}$$

$$\sum_{g\in\mathcal{G}_t} v^{\text{gen}}_{n,g,i} \leq \bar{V}^{\text{gen}}_{t,n,i}, \quad t\in\mathcal{T},\ n\in\mathcal{N},\ i\in\mathcal{I}, \tag{A.23}$$

$$v^{\text{tran}}_{l,i} \leq \bar{V}^{\text{tran}}_{l,i}, \quad l\in\mathcal{L},\ i\in\mathcal{I}, \tag{A.24}$$

$$v^{\text{storPW}}_{n,b,i} \leq \bar{V}^{\text{storPW}}_{n,b,i}, \quad b\in\mathcal{B}_n,\ n\in\mathcal{N},\ i\in\mathcal{I}, \tag{A.25}$$

$$v^{\text{storEN}}_{n,b,i} \leq \bar{V}^{\text{storEN}}_{n,b,i}, \quad b\in\mathcal{B}_n,\ n\in\mathcal{N},\ i\in\mathcal{I}. \tag{A.26}$$

Some storage technologies $b\in\mathcal{B}^{\dagger}\subseteq\mathcal{B}$ have dependencies between power and energy capacity:

$$v^{\text{storPW}}_{n,b,i} = \beta_b v^{\text{storEN}}_{n,b,i}, \quad b\in\mathcal{B}^{\dagger}\cap\mathcal{B}_n,\ n\in\mathcal{N},\ i\in\mathcal{I}. \tag{A.27}$$

Appendix B

Scenario Generation Results

This appendix presents the numerical results for the computational study.

Table B.1: Results for N=20 runs for the different scenario generation routines.

In Sample Stability		
Scenario Type	**Average**	**Relative St. Dev (%)**
R3	1.91+12	1.40
R5	1.93+12	2.73
R7	1.92+12	1.48
R10	1.93+12	0.94
M3	1.83+12	1.42
M5	1.85+12	2.42
M7	1.84+12	2.05
M10	1.85+12	1.59
ML3	1.83+12	1.84
ML5	1.84+12	1.90
ML7	1.85+12	1.15
ML10	1.85+12	1.43

Table B.2: Out-of-Sample results for N=40 scenarios for the different scenario generation routines when the investment decisions are already locked.

Out-of-Sample Stability		
Scenario Type	**Average**	**Relative St. Dev (%)**
R3	2.13+12	6.45
R5	2.00+12	1.48
R7	1.99+12	1.73
R10	1.98+12	2.94
M3	2.05+12	2.46
M5	2.02+12	2.22
M7	2.00+12	2.80
M10	1.98+12	0.96
ML3	2.60+12	8.47
ML5	2.46+12	5.61
ML7	2.24+12	5.78
ML10	2.23+12	3.95

Table B.3: Average generated installed capacity and annual production for Solar power for the respective Scenario Generation Routines.

Solar	Avg. Generated Installed Capacity (GW)				Relative St. Dev (%)			
Type	**2025**	**2030**	**2035**	**2040**	**2025**	**2030**	**2035**	**2040**
R3	2.55+05	2.81+05	2.86+05	2.86+05	9.70	10.12	9.34	9.34
R5	2.45+05	2.78+05	2.81+05	2.81+05	8.43	7.87	7.61	7.62
R7	2.38+05	2.65+05	2.67+05	2.67+05	12.11	12.94	13.04	13.04
R10	2.54+05	2.81+05	2.82+05	2.82+05	5.30	5.99	6.05	6.05
M3	2.40+05	2.59+05	2.65+05	2.65+05	7.66	6.56	6.21	6.21
M5	2.43+05	2.68+05	2.73+05	2.73+05	5.26	4.75	5.39	5.40
M7	2.43+05	2.65+05	2.69+05	2.69+05	4.18	4.00	3.59	3.59
M10	2.43+05	2.62+05	2.64+05	2.64+05	7.26	8.24	8.33	8.33
ML3	2.16+05	2.35+05	2.37+05	2.37+05	12.76	12.86	12.98	12.98
ML5	2.19+05	2.36+05	2.39+05	2.39+05	5.10	5.74	5.40	5.40
ML7	2.19+05	2.34+05	2.37+05	2.37+05	4.7	5.4	4.7	4.7
ML10	2.14+05	2.32+05	2.33+05	2.33+05	10.8	11.7	11.9	11.9
	Avg. Annual Production (TWh)				Relative St. Dev (%)			
R3	3.27+05	3.58+05	3.66+05	3.70+05	13.2	14.2	10.6	12.5
R5	3.08+05	3.55+05	3.57+05	3.61+05	11.7	8.2	8.6	9.9
R7	3.02+05	3.40+05	3.44+05	3.40+05	14.2	13.7	14.5	14.9
R10	3.26+05	3.66+05	3.66+05	3.66+05	7.4	7.4	8.4	6.6
M3	3.14+05	3.37+05	3.46+05	3.49+05	9.5	8.6	7.3	7.7
M5	3.14+05	3.49+05	3.56+05	3.58+05	7.2	5.0	6.6	6.3
M7	3.15+05	3.45+05	3.54+05	3.49+05	6.0	5.4	4.9	4.7
M10	3.15+05	3.44+05	3.46+05	3.48+05	8.3	9.0	9.7	9.0
ML3	2.47+05	2.77+05	2.74+05	2.72+05	15.3	15.6	16.1	15.1
ML5	2.50+05	2.73+05	2.76+05	2.77+05	7.1	8.3	6.7	7.2
ML7	2.53+05	2.71+05	2.75+05	2.76+05	6.3	6.9	5.7	5.8
ML10	2.45+05	2.68+05	2.70+05	2.70+05	11.9	13.5	12.7	13.3

Table B.4: Average generated installed capacity and annual production for Wind Offshore power for the respective Scenario Generation Routines.

Wind Offshore	Avg. Generated Installed Capacity (GW)				Relative St. Dev (%)			
Type	**2025**	**2030**	**2035**	**2040**	**2025**	**2030**	**2035**	**2040**
R3	1.81+04	1.81+04	4.90+04	4,90+04	6.2	6.2	28.8	28.8
R5	1,83+04	1,83+04	4,90+04	4,90+04	4.6	4.6	28.4	28.4
R7	1.81+04	1.81+04	4.54+04	4.54+04	4.4	4.4	26.5	26.5
R10	1.79+04	1.79+04	4.75+04	4.75+04	2.8	2.8	25.4	25.4
M3	1.80+04	1.80+04	4.51+04	4.51+04	4.1	4.1	26.7	26.7
M5	1.82+04	1.82+04	3.98+04	3.98+04	3.5	3.5	23.8	23.8
M7	1.79+04	1.79+04	4.41+04	4.41+04	2.1	2.1	22.7	22.7
M10	1.78+04	1.78+04	3.65+04	3.65+04	2.4	2.4	20.3	20.3
ML3	1.87+04	1.87+04	4.62+04	4.62+04	5.7	5.7	33.4	33.4
ML5	1.82+04	1.82+04	4.75+04	4.75+04	3.8	3.8	20.3	20.3
ML7	1.84+04	1.84+04	4.56+04	4.56+04	4.0	4.0	28.9	28.9
ML10	1.80+04	1.80+04	4.80+04	4.80+04	2.2	2.2	21.2	21.2
	Avg. Annual Production (TWh)				Relative St. Dev (%)			
R3	5.20+04	5.41+04	1.74+05	1.81+05	12.5	15.1	33.9	32.3
R5	5.21+04	5.31+04	1.77+05	1.80+05	5.4	11.1	30.7	32.5
R7	5.08+04	5.24+04	1.64+05	1.65+05	9.1	8.4	29.3	29.2
R10	4.91+04	5.15+04	1.70+05	1.74+05	5.1	8.7	28.4	27.5
M3	5.35+04	5.68+04	1.68+05	1.71+05	7.3	6.8	29.4	31.1
M5	5.69+04	5.76+04	1.48+05	1.50+05	5.5	6.9	25.5	28.0
M7	5.31+04	5.61+04	1.66+05	1.72+05	3.0	4.5	24.9	25.2
M10	5.30+04	5.52+04	1.34+05	1.36+05	4.6	5.7	21.9	22.8
ML3	5.56+04	5.99+04	1.73+05	1.77+05	9.7	11.3	37.4	38.1
ML5	5.38+04	5.73+04	1.79+05	1.79+05	9.7	7.1	21.6	22.9
ML7	5.50+04	5.70+04	1.69+05	1.70+05	6.1	8.1	31.1	32.6
ML10	5.31+04	5.55+04	1.80+05	1.81+05	5.6	6.2	23.1	24.1

Table B.5: Average generated installed capacity and annual production for Wind Onshore power for the respective Scenario Generation Routines.

Wind Onshore	Avg. Generated Installed Capacity (GW)				Relative St. Dev (%)			
Type	**2025**	**2030**	**2035**	**2040**	**2025**	**2030**	**2035**	**2040**
R3	4.22+05	4.93+05	4.99+05	4.99+05	6.5	7.0	7.1	7.1
R5	4.41+05	4.96+05	5.02+05	5.02+05	6.1	5.3	6.4	6.4
R7	4.44+05	5.01+05	5.10+05	5.10+05	7.2	5.6	5.3	5.3
R10	4.37+05	4.96+05	4.99+05	4.99+05	4.1	4.5	4.7	4.7
M3	4.58+05	5.29+05	5.43+05	5.43+05	6.9	3.7	4.6	4.6
M5	4.59+05	5.30+05	5.39+05	5.39+05	4.1	4.0	4.6	4.6
M7	4.57+05	5.30+05	5.35+05	5.35+05	3.0	3.5	3.7	3.7
M10	4.59+05	5.41+05	5.46+05	5.46+05	3.1	2.6	3.2	3.2
ML3	4.57+05	5.31+05	5.41+05	5.41+05	6.4	4.7	5.1	5.1
ML5	4.65+05	5.31+05	5.36+05	5.36+05	3.2	4.2	4.0	4.0
ML7	4.63+05	5.32+05	5.38+05	5.38+05	4.1	4.5	5.1	5.1
ML10	4.63+05	5.33+05	5.36+05	5.36+05	3.6	3.1	3.1	3.1
	Avg. Annual Production (TWh)				Relative St. Dev (%)			
R3	9.43+05	1.11+06	1.08+06	1.09+06	10.9	10.7	8.7	9.9
R5	9.75+05	1.08+06	1.10+06	1.12+06	9.7	9.2	8.6	8.9
R7	9.65+05	1.10+06	1.14+06	1.14+06	10.5	8.4	6.2	7.3
R10	9.44+05	1.09+06	1.10+06	1.12+06	5.9	6.5	6.3	8.2
M3	1.06+06	1.25+06	1.28+06	1.28+06	8.3	7.2	8.3	6.3
M5	1.08+06	1.25+06	1.26+06	1.26+06	4.8	5.4	6.5	5.8
M7	1.06+06	1.25+06	1.26+06	1.29+06	4.2	4.4	4.3	5.0
M10	1.07+06	1.27+06	1.29+06	1.28+06	4.2	3.3	3.7	3.7
ML3	1.04+06	1.26+06	1.27+06	1.26+06	10.0	7.8	7.5	10.8
ML5	1.07+06	1.24+06	1.26+06	1.25+06	6.7	6.8	7.8	7.1
ML7	1.05+06	1.24+06	1.24+06	1.25+06	5.0	5.9	7.2	6.3
ML10	1.07+06	1.24+06	1.26+06	1.25+06	5.8	3.9	3.9	3.7

Table B.6: Average generated installed capacity and annual production for Hydro Run-of-the-river power for the respective Scenario Generation Routines.

Hydro Run-of-the-river	Avg. Generated Installed Capacity (GW)				Relative St. Dev (%)			
Type	**2025**	**2030**	**2035**	**2040**	**2025**	**2030**	**2035**	**2040**
R3	8.09+04	8.27+04	8.30+04	8.30+04	2.0	0.7	0.9	0.9
R5	8.16+04	8.28+04	8.30+04	8.30+04	1.9	0.5	0.6	0.6
R7	8.21+04	8.28+04	8.30+04	8.30+04	0.6	0.5	0.6	0.6
R10	8.19+04	8.30+04	8.31+04	8.31+04	1.1	0.6	0.6	0.6
M3	8.05+04	8.27+04	8.33+04	8.33+04	1.8	0.6	0.5	0.5
M5	8.01+04	8.32+04	8.34+04	8.34+04	2.5	0.5	0.7	0.7
M7	8.12+04	8.32+04	8.35+04	8.35+04	1.7	0.6	0.6	0.6
M10	8.06+04	8.31+04	8.33+04	8.33+04	2.2	0.4	0.4	0.4
ML3	8.11+04	8.27+04	8.29+04	8.30+04	2.1	0.7	0.6	0.6
ML5	8.17+04	8.30+04	8.32+04	8.32+04	1.7	0.4	0.4	0.4
ML7	8.14+04	8.31+04	8.32+04	8.32+04	2.4	0.4	0.5	0.5
ML10	8.19+04	8.31+04	8.31+04	8.31+04	2.0	0.3	0.4	0.4
	Avg. Annual Production (TWh)				Relative St. Dev (%)			
R3	2.98+05	2.90+05	2.93+05	2.92+05	4.9	4.0	2.9	2.6
R5	2.98+05	2.92+05	2.91+05	2.90+05	4.1	2.2	2.3	3.4
R7	3.01+05	2.93+05	2.93+05	2.92+05	2.6	2.5	2.3	2.0
R10	3.00+05	2.91+05	2.93+05	2.91+05	2.4	1.7	2.2	2.2
M3	2.88+05	2.83+05	2.83+05	2.85+05	3.5	3.0	3.1	2.9
M5	2.87+05	2.83+05	2.82+05	2.82+05	5.7	3.0	2.5	3.2
M7	2.92+05	2.83+05	2.83+05	2.81+05	2.5	2.2	2.5	2.2
M10	2.89+05	2.84+05	2.82+05	2.83+05	4.0	2.5	1.9	2.4
ML3	3.00+05	2.91+05	2.88+05	2.92+05	4.0	2.7	2.2	2.4
ML5	3.02+05	2.92+05	2.91+05	2.94+05	3.8	1.9	3.1	1.8
ML7	3.02+05	2.92+05	2.91+05	2.92+05	4.3	1.6	2.0	1.6
ML10	3.02+05	2.92+05	2.92+05	2.91+05	2.9	1.2	1.6	1.5

Table B.7: Results for N=20 runs for each model in the reduced EMPIRE-model. Each model has been run against a total of 500 randomly generated scenarios equal for the different scenario generation routines.

In Sample Stability		
Scenario Type	**Average**	**Relative St. Dev (%)**
RR10	6.12+11	1.7
RR50	6.19+11	0.8
RR100	6.19+11	0.7
RR200	6.19+11	0.6
Out-of-Sample Stability		
RR10	6.38E+11	1.54
RR50	6.22E+11	0.48
RR100	6.21E+11	0.27
RR200	6.20E+11	0.13

Table B.8: Average generated installed capacity and annual production for Solar power for the reduced EMPIRE-model.

Solar	Avg. Generated Installed Capacity (GW)				Relative St. Dev (%)			
Type	**2025**	**2030**	**2035**	**2040**	**2025**	**2030**	**2035**	**2040**
RR10	6.90+04	7.30+04	7.35+04	7.35+04	7.5	12.3	12.9	12.9
RR50	6.73+04	6.95+04	6.95+04	6.95+04	7.9	8.9	8.9	8.9
RR100	6.72+04	6.85+04	6.85+04	6.85+04	4.1	6.4	6.4	6.4
RR200	6.75+04	6.82+04	6.82+04	6.82+04	4.5	4.6	4.6	4.6
	Avg. Annual Production (TWh)				Relative St. Dev (%)			
RR10	7.67+04	8.08+04	8.13+04	8.18+04	9.9	14.8	15.1	16.8
RR50	7.36+04	7.67+04	7.71+04	7.70+04	8.8	10.6	10.2	10.3
RR100	7.40+04	7.59+04	7.58+04	7.56+04	4.8	7.5	7.4	6.7
RR200	7.45+04	7.52+04	7.52+04	7.52+04	4.5	4.5	5.1	4.9

Table B.9: Average generated installed capacity and annual production for Wind Offshore power for the reduced EMPIRE-model.

Wind Offshore	Avg. Generated Installed Capacity (GW)				Relative St. Dev (%)			
Type	**2025**	**2030**	**2035**	**2040**	**2025**	**2030**	**2035**	**2040**
RR10	7.56+03	7.56+03	1.15+04	1.15+04	0.0	0.0	47.3	47.3
RR50	7.56+03	7.56+03	1.27+04	1.27+04	0.0	0.0	45.1	45.1
RR100	7.56+03	7.56+03	1.25+04	1.25+04	0.0	0.0	35.4	35.4
RR200	7.56+03	7.56+03	1.04+04	1.04+04	0.0	0.0	27.8	27.8
	Avg. Annual Production (TWh)				Relative St. Dev (%)			
RR10	2.12+04	2.19+04	3.76+04	3.71+04	9.5	9.0	61.5	56.1
RR50	2.13+04	2.18+04	4.22+04	4.21+04	6.9	4.4	53.9	54.6
RR100	2.15+04	2.17+04	4.15+04	4.14+04	2.8	3.1	42.7	42.3
RR200	2.15+04	2.17+04	3.30+04	3.30+04	2.3	1.7	34.6	35.2

Table B.10: Average generated installed capacity and annual production for Wind Onshore power for the reduced EMPIRE-model.

Wind Onshore	Avg. Generated Installed Capacity (GW)				Relative St. Dev (%)			
Type	**2025**	**2030**	**2035**	**2040**	**2025**	**2030**	**2035**	**2040**
RR10	9.21+04	1.14+05	1.14+05	1.14+05	12.0	11.5	11.5	11.5
RR50	9.49+04	1.14+05	1.14+05	1.14+05	7.3	7.9	7.9	7.9
RR100	9.28+0	1.12+05	1.12+05	1.12+05	5.3	7.1	7.1	7.1
RR200	9.20+04	1.15+05	1.15+05	1.15+05	5.8	4.1	4.1	4.1
	Avg. Annual Production (TWh)				Relative St. Dev (%)			
RR10	1.69+05	2.25+05	2.22+05	2.21+05	20.2	17.5	18.1	17.0
RR50	1.75+05	2.22+05	2.20+05	2.18+05	12.1	10.2	10.1	9.4
RR100	1.71+05	2.18+05	2.18+05	2.18+05	8.7	10.2	8.9	8.8
RR200	1.70+05	2.22+05	2.24+05	2.23+05	8.1	5.6	5.3	5.0

Table B.11: Average generated installed capacity and annual production for Hydro Run-of-the-River power for the reduced EMPIRE-model.

Hydro Run-of-the-River	Avg. Generated Installed Capacity (GW)				Relative St. Dev (%)			
Type	**2025**	**2030**	**2035**	**2040**	**2025**	**2030**	**2035**	**2040**
RR10	2.50+04	2.50+04	2.50+04	2.50+04	0.0	0.0	0.0	0.0
RR50	2.50+04	2.50+04	2.50+04	2.50+04	0.0	0.0	0.0	0.0
RR100	2.50+04	2.50+04	2.50+04	2.50+04	0.0	0.0	0.0	0.0
RR200	2.50+04	2.50+04	2.50+04	2.50+04	0.0	0.0	0.0	0.0
	Avg. Annual Production (TWh)				Relative St. Dev (%)			
RR10	1.26+05	1.27+05	1.26+05	1.26+05	3.4	3.2	3.8	2.7
RR50	1.26+05	1.26+05	1.27+05	1.27+05	0.9	1.7	1.5	1.7
RR100	1.25+05	1.27+05	1.27+05	1.27+05	1.0	1.2	1.0	0.8
RR200	1.26+05	1.27+05	1.27+05	1.27+05	0.7	0.8	0.9	0.8